AD NUMBER

AD857831

NEW LIMITATION CHANGE

TO

Approved for public release, distribution unlimited

FROM

Distribution authorized to U.S. Gov't. agencies only; Administrative/Operational Use; 01 APR 1969. Other requests shall be referred to Naval Electronics Lab Center, San Diego, CA.

AUTHORITY

USNELC ltr, 22 Aug 1974

LUNEBERG LENS ANTENNA - TESTING FOR ECM APPLICATION

Appropriate receiving and display techniques permit use of lens in direction-finding system

M. B. Bryant and B. R. Hunt Research and Development Report 1 April 1969

EACH TRANSMITTAL OF THIS DOCUMENT OUTSIDE THE AGENCIES OF THE U. S. GOVERNMENT MUST HAVE PRIOR APPROVAL OF NELC.

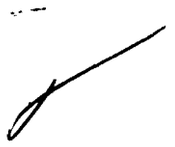

3

PROBLEM

Investigate the Luneberg lens for use as an *X*-band antenna capable of providing instantaneous reception and accurate direction-finding (DF) over 360° azimuth. More specifically, conduct the investigation as follows:

1. **Design a practical feed horn for use with the lens.**
2. **Optimize the lens for high-signal transmissibility.**
3. **Optimize the lens feed-horn system to obtain high gain, narrow beamwidths, low sidelobes, and acceptance of multiple polarizations.**
4. **Develop an applicable receiving technique to test the feasibility of using the lens in a DF system and determine the merits of such a system.**
5. **Theoretically, consider a specific DF-system configuration which can be used to meet Fleet needs.**

RESULTS

1. Armstrong Cork developed the 44- and 18-inch Luneberg lens antennas for NELC with characteristics suitable for a multibeam, common-aperture direction finder at *X*-band.

2. The gain and beamshaping properties of the 18-inch Luneberg and 24-inch constant-K lenses are comparable to those of the 44-inch Luneberg lens. Tests also showed both lenses can be optimized to receive all polarizations.

3. The optimum feed-horn array was determined to be one which optimized the lens' response to all polarizations and permitted close spacing of the beam centers.*

- The lens was found to transmit either vertical or horizontal polarization; however, the NELC-designed *E*-plane sectoral feed horn degraded the cross-polarizing component.
- Canting the NELC horn at 45° still left it susceptible to degradation by the reverse 45° polarization.
- Pattern measurements with a spiral (small cavity-backed) feed horn indicated satisfactory response to vertical, horizontal, and 45° polarization modes.

---

* *Maximum spacing is dictated by the desired DF accuracy, while minimum spacing is a function of of the physical size of the feed horn and circumference of the lens. DF accuracy is greatest at minimum spacing.*

4. A four-channel DF receiver was built to test the operation of the Luneberg lens. Four crystal-video channels, logic-thresholding techniques, and a cathode-ray tube (CRT) display were used to determine signal bearing on a pulse-by-pulse basis. Controlled tests conducted at 9 GHz, showed breadboard sensitivities of -55 to -57 dBm and bearing errors of about ± 4.5° over an azimuth sector of 27°. Because four *E*-plane sectoral feeds (canted at 45° on 9° centers around the lens) were used, the source for the tests was set for vertical polarization.

5. Techniques and performance predictions for a practical DF system involving the Luneberg lens were evolved.

RECOMMENDATIONS

1. Use a properly shielded Luneberg lens to generate the response patterns of beams which lie at the periphery of the 120°-azimuth coverage of a single lens.

2. Generate multibeam patterns for the constant-K lens. (Space feed horns 5°-9° apart.)

3. Implement and evaluate a direction finder using a single Luneberg lens with *E*-plane sectoral feeds and an omniantenna for sidelobe suppression.

ADMINISTRATIVE INFORMATION

This investigation was performed under SF11.151.001, Task 09251 (NELC G203), by members of the EM Surveillance and Countermeasures Division from March 1967 to April 1968. Contractual efforts with Emerson and Cuming Inc., and Armstrong Cork Company covered March to June 1965 and May 1966 to January 1968, respectively. The report was approved for publication 1 April 1969.

CONTENTS

ILLUSTRATIONS

ILLUSTRATIONS (Continued)

ILLUSTRATIONS (Continued)

INTRODUCTION

Development of the Luneberg lens was conceived principally as an antenna development, aimed at increasing the gain, narrowing the beamwidth, and reducing the sidelobes of the lens to levels that are comparatively better than those furnished by other microwave-ECM antennas. Once achieved, these improved characteristics, along with the multibeam capability of the lens, were to be optimized and explored for DF-system applications. A constant-K lens was also designed for comparative purposes and evaluated as part of the subject task. These studies and tests are discussed in this report.

In addition, several efforts – project SHORTSTOP, ALQ-78, and NELC's passive EW-receiving system – are underway which, if successful, will alleviate some problems of low intercept probability and poor DF accuracy in microwave systems. Another approach involves combining the Luneberg (or constant-K) lens with the instantaneous frequency measurement (IFM) receiver to permit simultaneous wide-open surveillance in frequency and azimuth.

THEORY

Luneberg Lens

The dielectric Luneberg lens is capable of focusing an incident plane wave at a point on its opposite surface (fig. 1). This capability is caused by a gradation of the index of refraction, η, as a function radius; this is usually according to the relationship:

$$\eta = \sqrt{K - \left(\frac{r}{R}\right)^2} \qquad (1)$$

WHAT IS IT? THE LUNEBERG LENS IS A DIELECTRIC LENS WHOSE FOCUSING PROPERTIES TO A PLANE WAVE ARE ACHIEVED BY A SMOOTH GRADATION OF THE DIELECTRIC CONSTANT (K) FROM ONE AT THE LENS' SURFACE TO TWO AT THE CENTER. TO ACHIEVE THE SMOOTH GRADATION OF THE DIELECTRIC CONSTANT, LENSES ARE CONSTRUCTED BY A SPECIAL MIXING AND BLENDING PROCESS IN LIEU OF THE FORMER PROCESS OF BONDING CONCENTRIC, DIELECTRIC SHELLS.

$K = 2 - \frac{r^2}{R}$ WHERE R = LENS RADIAL LENGTH

$n = \sqrt{K} = \sqrt{2 - \frac{r^2}{R}}$ WHERE n = INDEX OF REFRACTION

AND r = ANY LENGTH MEASURED FROM CENTER

Figure 1. Luneberg lens description.

where K is the dielectric constant at the center of the lens, R, the radius of the lens; and r, the variation in R from the center.[1]

This is based on the relationship

$$\eta = \frac{c}{v}$$

where

$$c = \sqrt{\frac{1}{\mu_0 \epsilon_0}}$$

$$v = \sqrt{\frac{1}{\mu \epsilon}} \qquad (\mu_0 \cong \mu_0)$$

Thus

$$\eta = \sqrt{\frac{\epsilon}{\epsilon_0}} = \sqrt{K_r}$$

where K_r is the relative dielectric constant; μ, the permeability; and ϵ, the permittivity of the medium. According to equation (1), K_r for the Luneberg antenna equals $K - \left(\frac{r}{R}\right)^2$ where $K = 2$.

For a lens of practical importance, the focus for incident plane waves must lie outside the surface of the lens. Solutions for this special case[2] show that the maximum η (center-of-lens value) must be less than $\sqrt{K}$ or $\sqrt{2}$. The exact reduction from $\sqrt{2}$ is directly proportional to the focal length external to the lens.

Figure 2 shows a cylindrical lens with an incident plane wave. Rays from the plane wave are drawn through the lens and curved to illustrate external focusing of the rays on the opposite side of the lens. A study of the center and outer rays shows that while the outer rays must travel a greater path length to reach the focal point, they, theoretically, arrive at the focal point in phase with the center ray because of their faster velocity. This is because the point-by-point η for the path of the outer rays is lower than that for the center ray. Also, because of inability to smoothly grade the dielectric constant of the lens as required by formula, some divergence from the theoretical may be expected, resulting in phase errors at a given focus.

[1] *Superscript numbers denote references listed at the end of this report.*

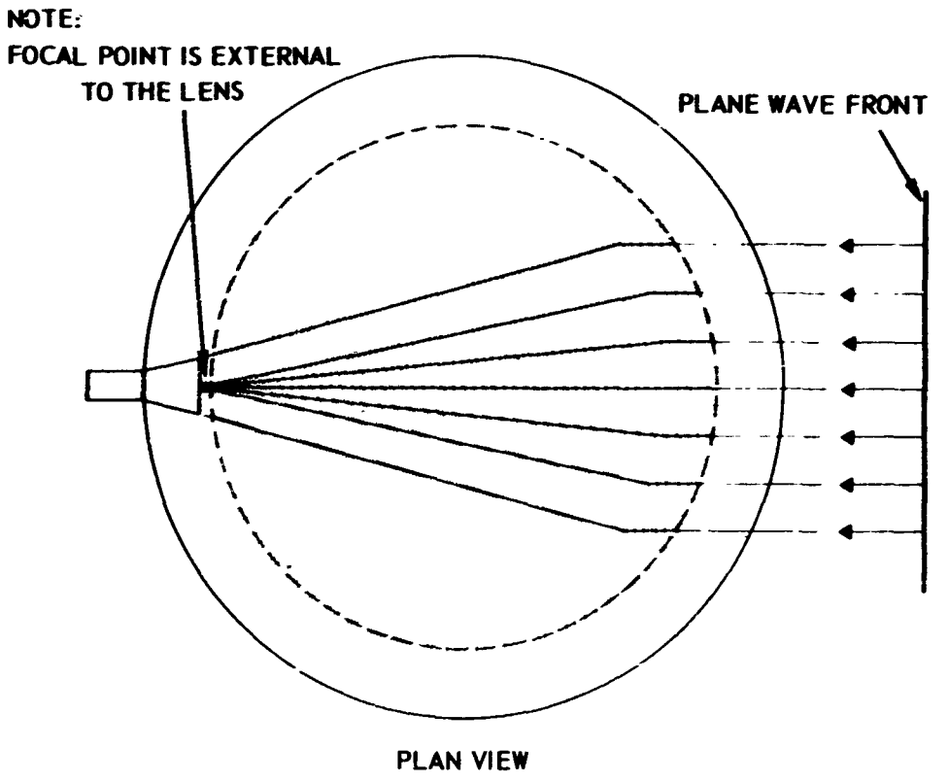

Figure 2. Ray focusing at feed horn.

Constant-K Lens

The constant-K lens differs from the Luneberg in that it is made from homgeneous material having a uniform dielectric constant.* Functionally, however, it is similar to the Luneberg since it focuses the rays of the incident plane waves on its opposite surface. In addition, the outer rays travel a longer path length than do the rays nearer the center. (Since the outer rays see the same K and travel at the same speed – over different path lengths – as the other rays nearer the center, phase aberrations at the focal point of the lens are common.)

Constant-K lenses are usually restricted in diameter to limit path-length differences across the aperture so phase aberrations are reduced. Cheston and Luoma[3] have shown that aberrations can also be reduced by properly choosing the dielectric constant of the lens material. They conclude that η^2 (typically chosen at 4) should be reduced below 3.5 to ensure external focusing and limit higher order aberrations.

**For this reason, it is easier to manufacture than the Luneberg lens*

The thick lens formula, relating the index of refraction and focal length, is as follows:

$$\frac{R'}{R} = \frac{\eta}{[2(\eta-1)]}$$

where R' is the focal radius measured from the center of the lens along the radial of interest, and R is the radius of the lens. The empirical formula,

$$\frac{R'}{R} = \frac{1}{\sqrt{2}} - \frac{K}{K-1}$$

has been found to be more useful.[3] This formula considers that the optimum dielectric constant for a surface focus lens is 3.5 and that K should be reduced below 3 5 to obtain focusing external to the lens. (The Luneberg and constant-K lenses in this program were focused externally.)

CONSTRUCTION DETAILS

Luneberg Lens

Construction of Luneberg lenses has been attempted by a number of methods, each intended to smoothly grade the dielectric constant of the lens material from 1 at the surface to less than (2) at the center. One method is a stepwise approximation[4] in which a number of uniform spherical shells, made of dielectric foam and varying slightly in dielectric constant, are bonded concentrically to approximate the required spherical gradation of K (fig. 3). The density of the dielectric foam determines K and is controllable during processing to a tolerance of 0.02 for K's between 1 and 2. (Cylindrical 2-D lenses are formed by cutting diametric sections from the spheres constructed in the above process.)

This type of construction is typical of that used by Emerson and Cuming Inc., Canton, Mass. Theoretically, with an infinite number of shells, the required gradation of K can be achieved smoothly, however, since the number of shells is finite, typically between 10 and 35, this does not result Therefore, these lenses are not as efficient as projected in theory due to reflections and defocusing by the shell boundaries. Nevertheless, lenses of this construction are widely used, especially as passive reflectors.

A second construction method, developed more recently by the Armstrong Cork Company, utilizes a blend of low density polystyrene foam and small aluminum slivers. The two materials are mixed to achieve an isotropic gradation of K (from 1 at the surface to less than (2) at the center) in cylindrical form. Slices are cut from the variable-index cylinder to fabricate 2-D lenses of the desired height, or cylindrical wedges are fashioned for use in the construction of spherical Luneberg lenses.

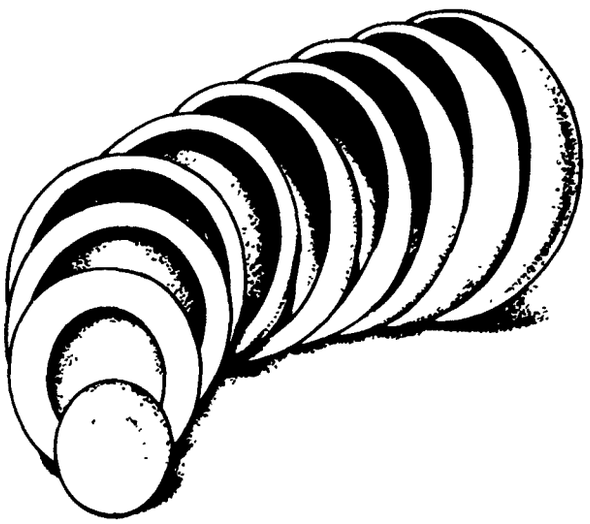

Figure 3 Hemispherical half-shell construction of stepped-index Luneberg lens.

While this approach seemingly approximates the Luneberg requirement more closely than the shell approach, it, too, is not completely loss-free because of dielectric-material losses and scatter losses by the aluminum slivers. Armstrong utilizes 50 and 90 mil slivers at *X*-band in an attempt to gain uniformity (isotropy) and reduce scatter losses.

Constant-K Lens

A 24-inch constant-K cylindrical lens was constructed from a plastic material (Rexolite 1422)* having a dielectric constant of 2.53. The plastic was carefully machined into a 24-inch cylindrical slice and mounted between conducting plates.

Both the Luneberg and constant-K cylindrical lenses were sandwiched between conducting plates (fig. 4). These plates purposely restrict the vertical-surveillance angle and provide a support for the lens material. A thin plastic radome is deposited over the entire structure for weatherproofing. Systems using either a Luneberg or constant-K lens will require at least three lenses for unobstructed surveillance over 360°. This is depicted in figures 5 and 6 for mast-top or around-the-mast mounting.

The vertical stacking of lenses as shown in figure 5 may also lend itself to simultaneous surveillance of several different frequency bands (with lenses and feeds designed for different frequency bands) Three such stacks would be required to obtain full surveillance over 360°.

---

* *Sold by Brand Rex Company, Division American ENKA CORPORATION, Willimantic, Connecticut 06224*

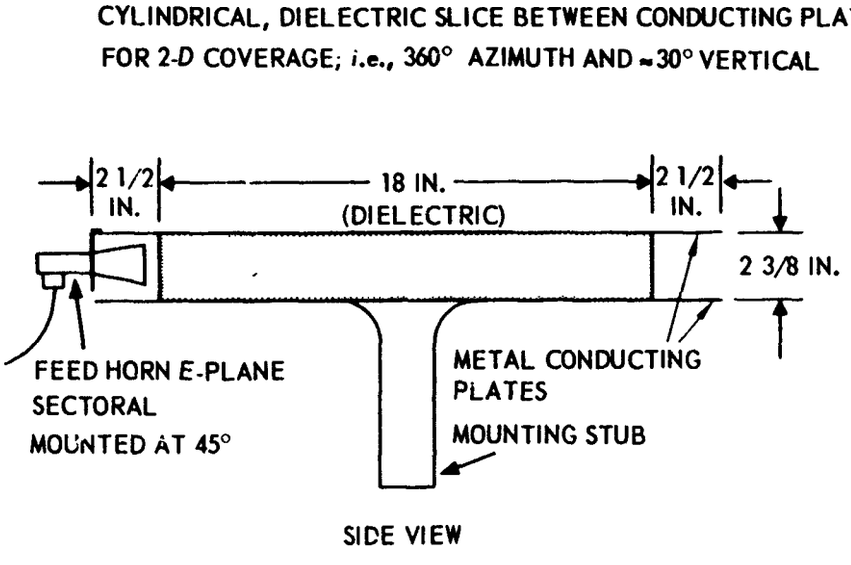

Figure 4. Luneberg lens configuration.

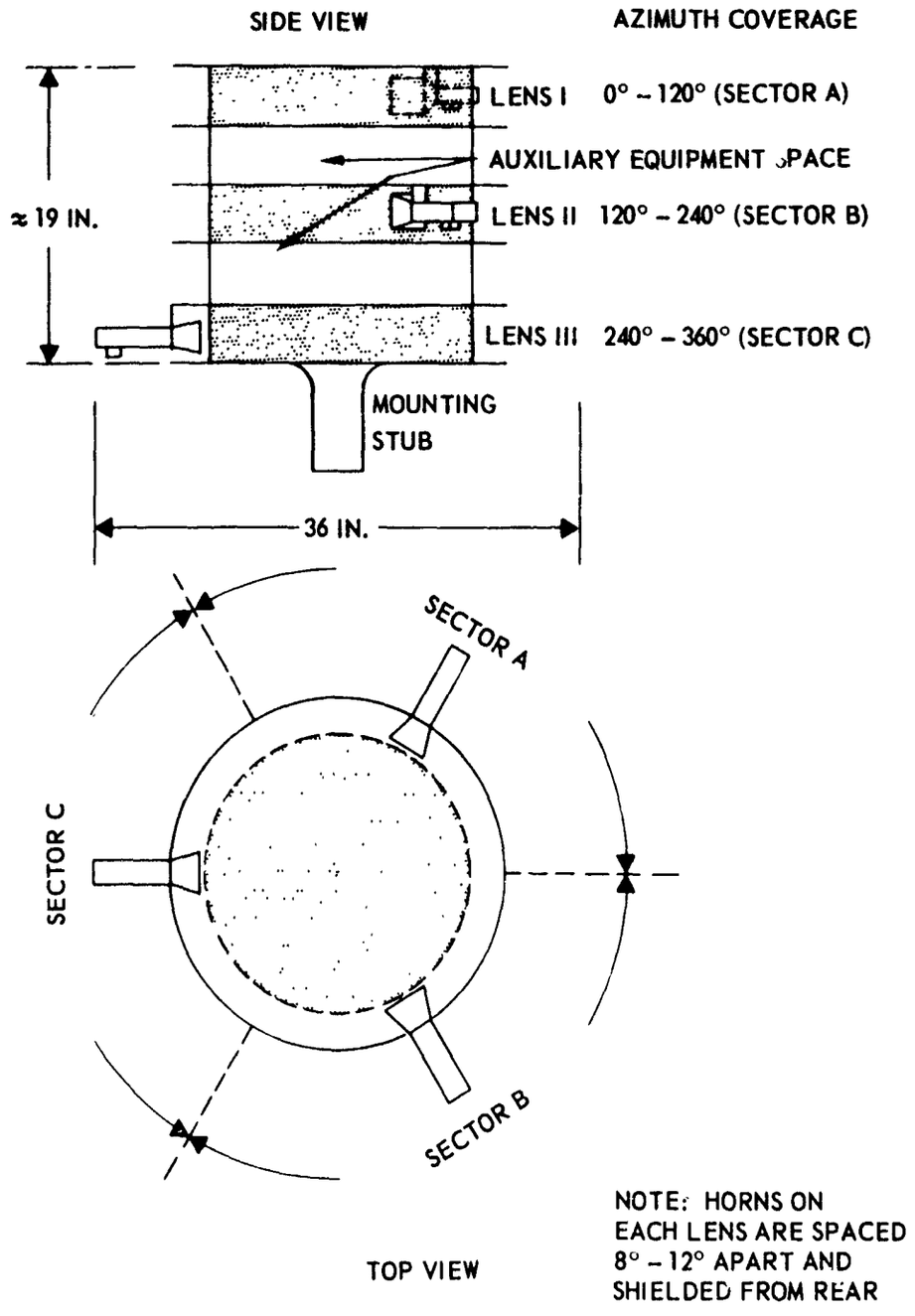

Figure 5 Mast-top-mounting configuration

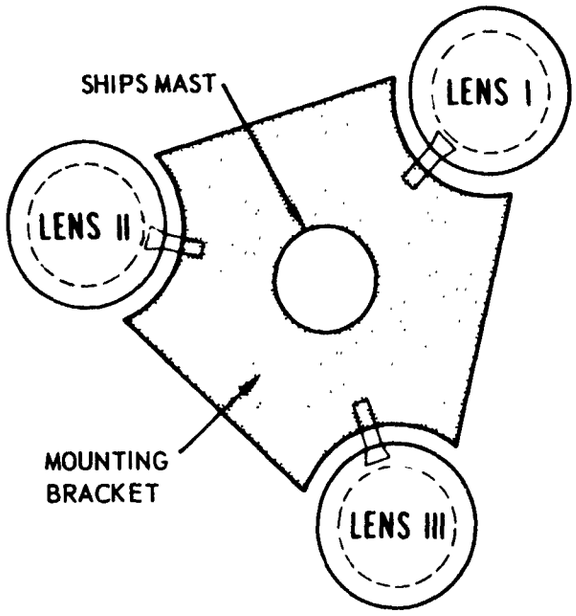

AZIMUTH COVERAGE

LENS I	LENS II	LENS III
0° – 120°	120° – 240°	240° – 360°

NOTE:
HORNS FOR EACH LENS ARE SPACED 8° – 12° APART AND SHIELDED FROM REAR

Figure 6 Around-mast-mounting configuration.

Developmental Contracts

In 1965, NELC began to consider the Luneberg lens for use as a simple, multibeam array which could provide instantaneous wide-open reception and bearing in ECM applications. It was hoped that the lens would provide sufficient gain to avoid the need for radio frequency (rf) preamplifiers. A survey at that time did not reveal a source with a lens suitable for purchase. Hence, NELC contracted for a specially built lens with the following specifications:

1. Absolute gain	23 dB minimum across the band
2. Sidelobes.	First sidelobes to be 20 dB or more below the main beam
3. Vertical beamwidth.	30° (preferred range 24° - 35°)
4. Horizontal beamwidth:	3° ± 5 percent at low end of band (7 5 GHz)
5. Frequency range:	7 5 - 10 5 GHz

Initial contract efforts were with Emerson and Cuming. The contract, N123 (953) 52715A, required the design, building, and delivery of the lens in 6 months. The 36-inch cylindrical 2-D lens, using stepped-refraction index construction, was obtained and tested at NELC near the end of 1965. The lens proved to be unsatisfactory, mainly because its sidelobes were excessively high. (At 8 and 12 GHz, sidelobes were unequal and often less than 10 dB below the main beam.) For this reason, the 36-inch lens was not considered for further testing. NELC then procured another lens. contract 123-5-56825A was let with Armstrong Cork Company of Lancaster, Pennsylvania, for a 44-inch lens using a smooth, continuously-variable index of refraction construction. Tests during 1967 with the trial 44-inch lens, and an 18-inch lens also purchased from Armstrong, were satisfactory, although not entirely up to contract specifications.

FEED HORNS

An integral part of the lens system is the feed horn which collects energy focused by the lens. It also exerts some influence on overall response because of its beam pattern and radial position relative to the focus of the lens. NELC used three different feed horns during its testing program – cavity-backed spirals, *E*-plane sectoral horns (figs. 7-8), and a Narda type 640 standard-gain horn.

During testing of the 44-inch lens, the type 640 and *E*-plane sectoral horns were used, usually with one horn connected to the lens. During system testing of the 18-inch lens as many as seven feed horns were connected (fig. 9). Tests with a spiral feed were also made on the 18-inch lens with one spiral at a time connected to the lens.

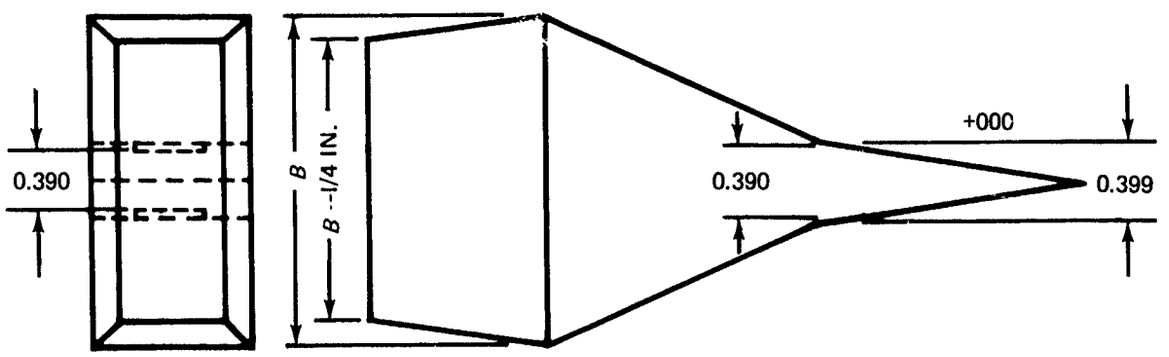

B = THICKNESS OF LENS MINUS 1/8 IN.
B = 1 3/4 IN.
B – = 1 1/2 IN.

Figure 7. Feed-horn beam-tapering lens (teflon-dielectric loading)

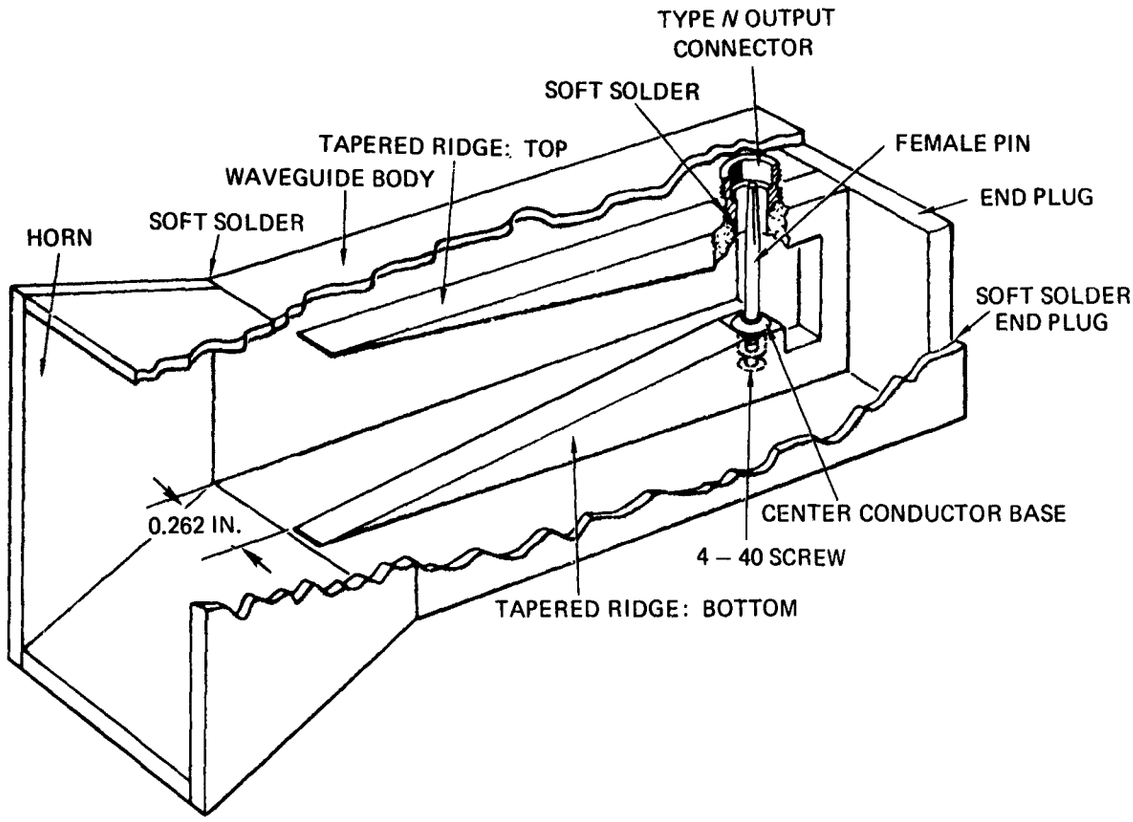

Figure 8. X-band antenna feed-horn assembly

The cavity-backed spirals, Model ASN 1226A, were built by American Electronic Laboratory (AEL), Pennsylvania. Patterns of response of the spiral at 9 GHz are shown in figure 10. Similarly, figure 11 shows the 10-GHz response of the *E*-plane sectoral feeds. The *E*-plane sectoral horns were designed and built, in-house, by the NELC model range personnel specifically for the Luneberg project. (This was also the basic feed used by Armstrong Cork in optimizing and evaluating its lens development.)

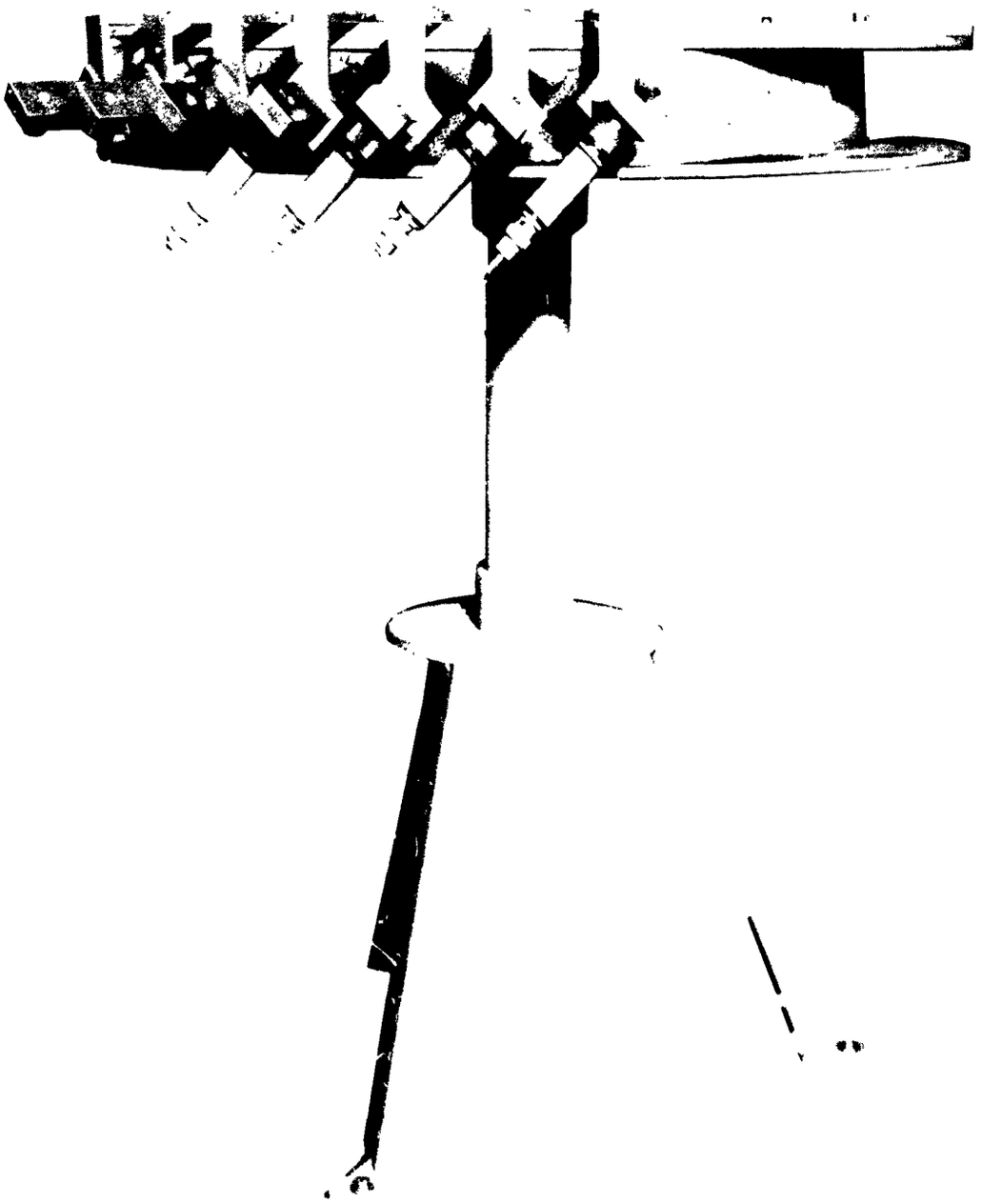

Figure 9. Luneberg 18-inch lens showing seven feed horns mounted for testing.

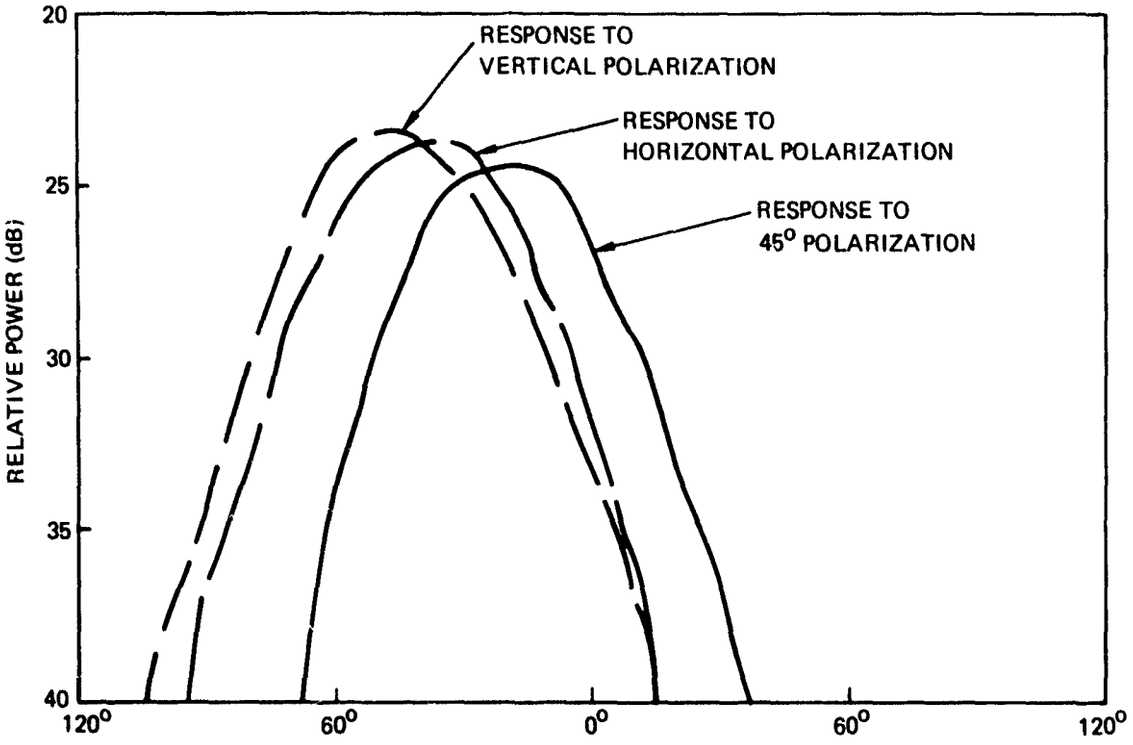

Figure 10. Azimuth pattern at 9 GHz (AEL spiral ASN 1226A).

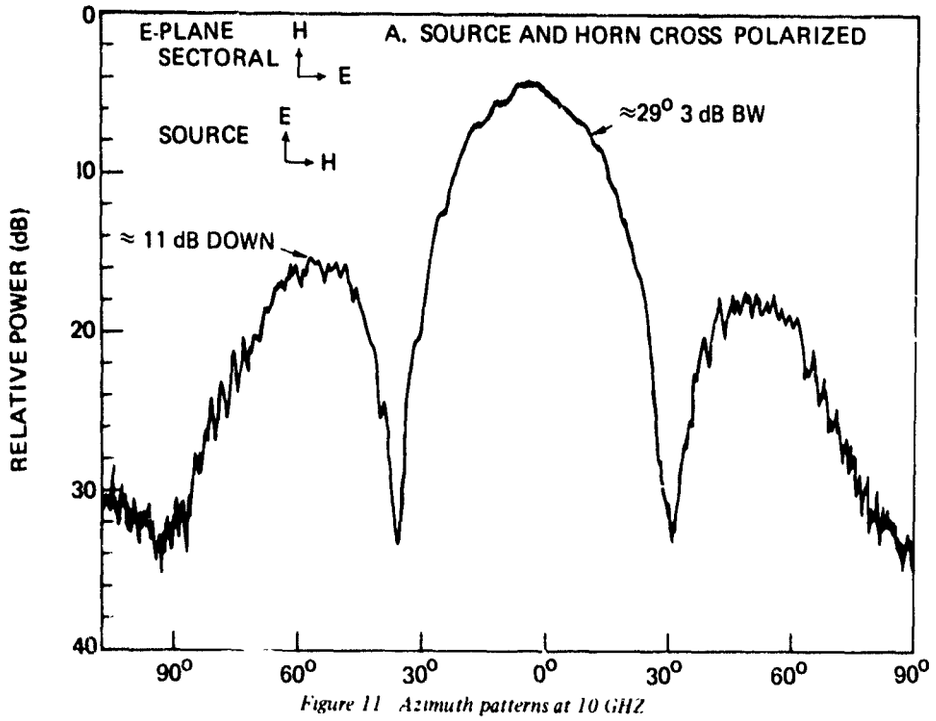

Figure 11 Azimuth patterns at 10 GHZ

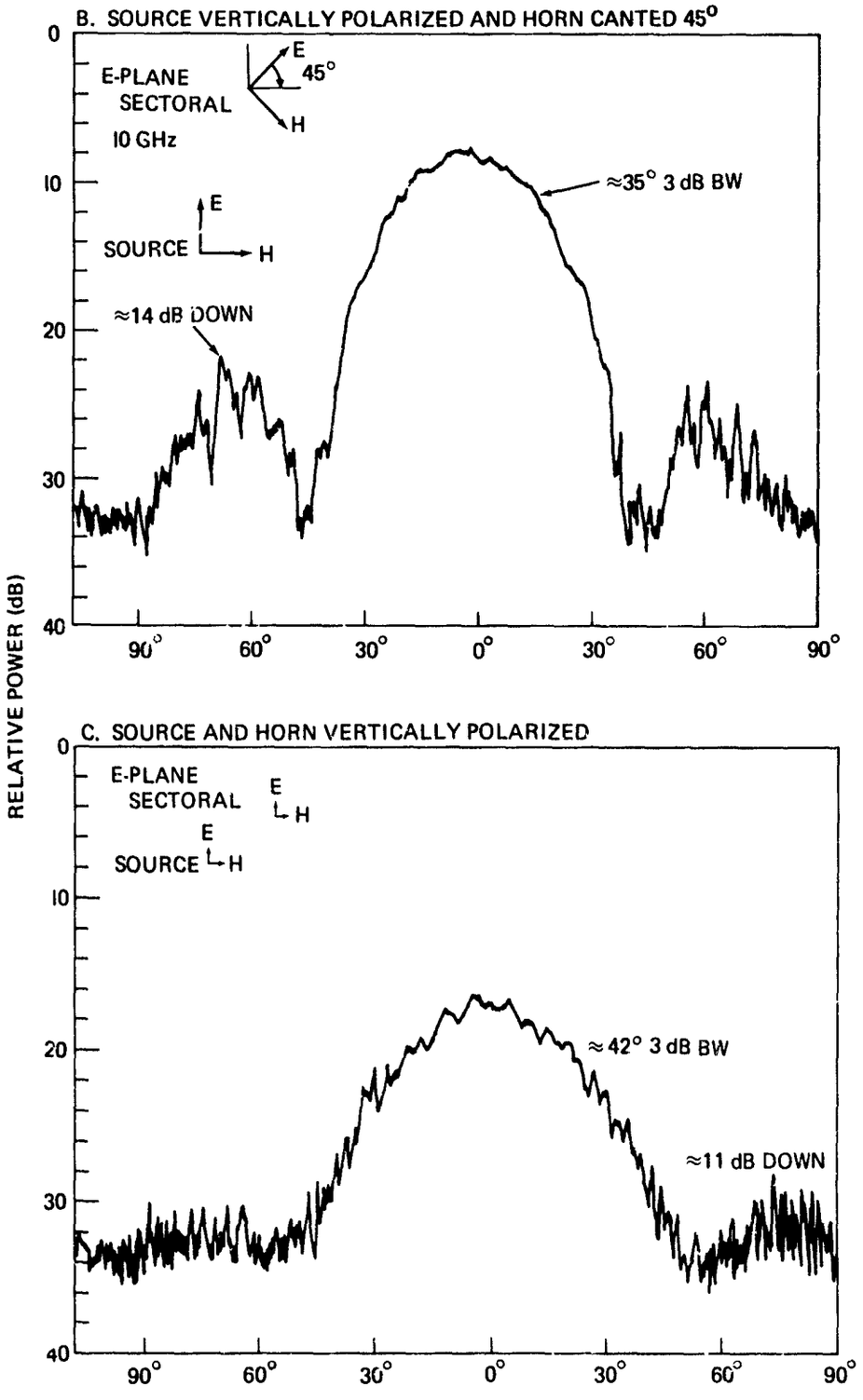

Figure 11 (Continued)

OPTIMIZED PATTERNS

Comparative Azimuth and Elevation Responses

Figure 12 shows the 10-GHz azimuth responses of the 44- and 18-inch lenses. Both lenses used vertically-polarized *E*-plane sectoral feeds placed at optimum focal points.

The total gains and beamwidths of the lenses are observed to be within 2 dB, while the first sidelobes of the 18-inch lens are approximately 6 dB further down. Comparatively, the 18-inch lens exhibits a better azimuth response.

Figure 13 shows the responses of the lenses elevated 15° above boresight. Both show a reduction in total gain of about 3 dB and a change in sidelobes; neither change is serious. The 18-inch lens is observed to exhibit less change in the balance of its first sidelobes with elevation. Elevation patterns of the two lenses are similar and help explain the near-equal reduction in total gain for the given elevation (fig. 14).

Figure 15 permits a comparative study of the azimuth response of the 18-inch lens at three frequencies. (Figure 16 gives a similar study for the 44-inch lens.) These patterns when compared to those at 10 GHz, indicate the adequacy of the lenses' response over the frequency band of interest.

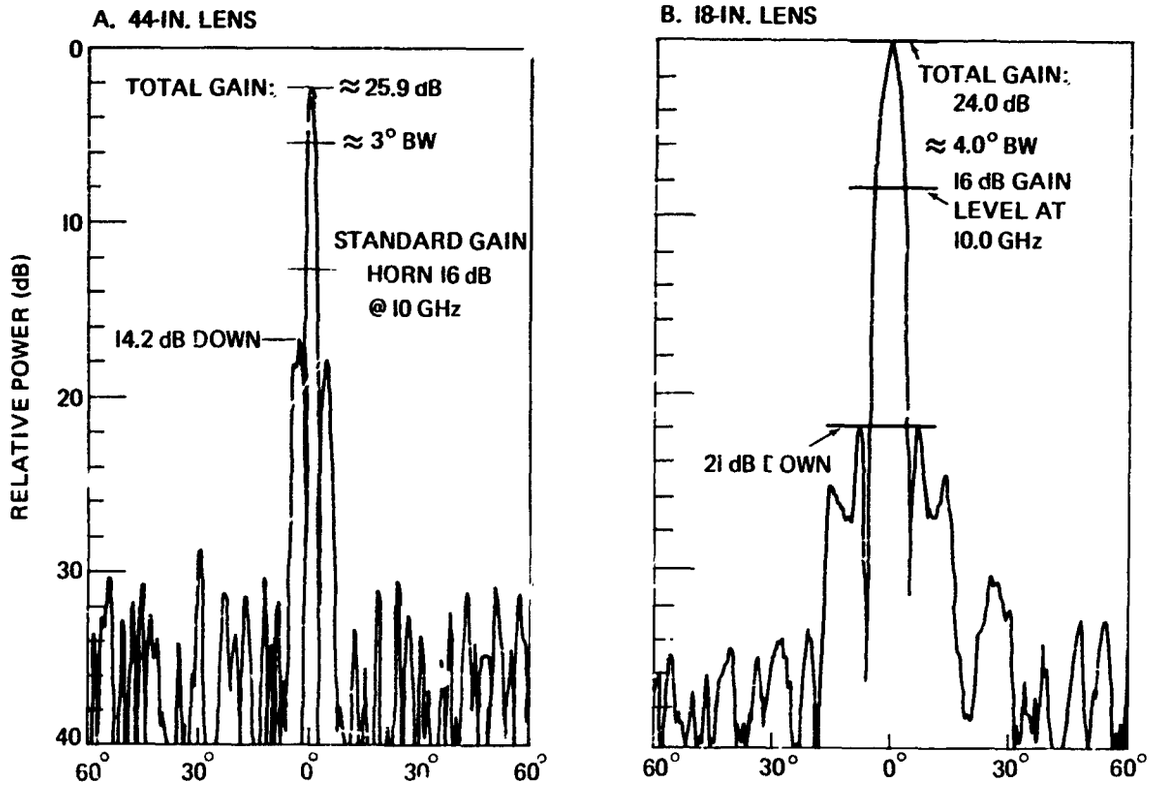

Figure 12. Sectoral feed and source vertically polarized for 10-GHz azimuth patterns at 0° elevation.

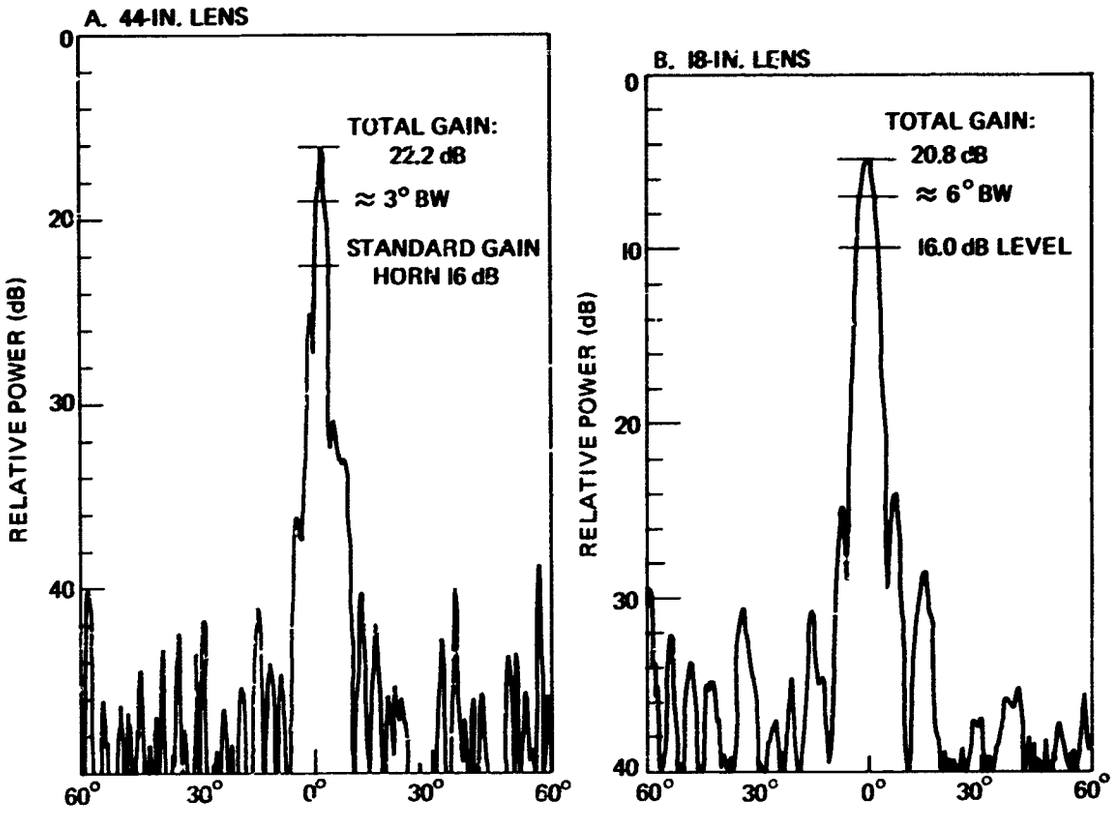

Figure 13. Sectoral feed and source vertically polarized for 10-GHz azimuth patterns at 15° elevation.

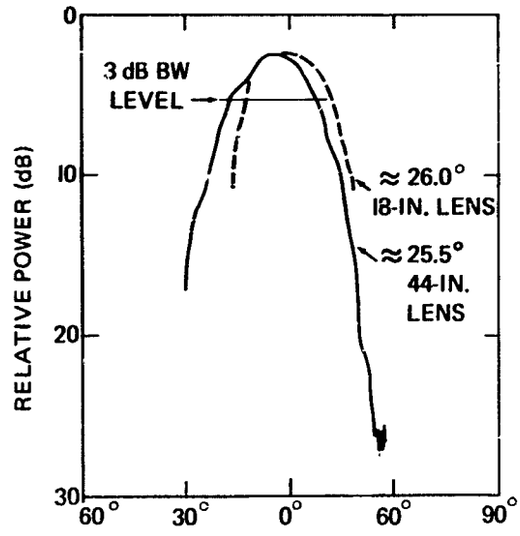

Figure 14. Sectoral feed and source vertically polarized for 10-GHz elevation pattern at 0° azimuth

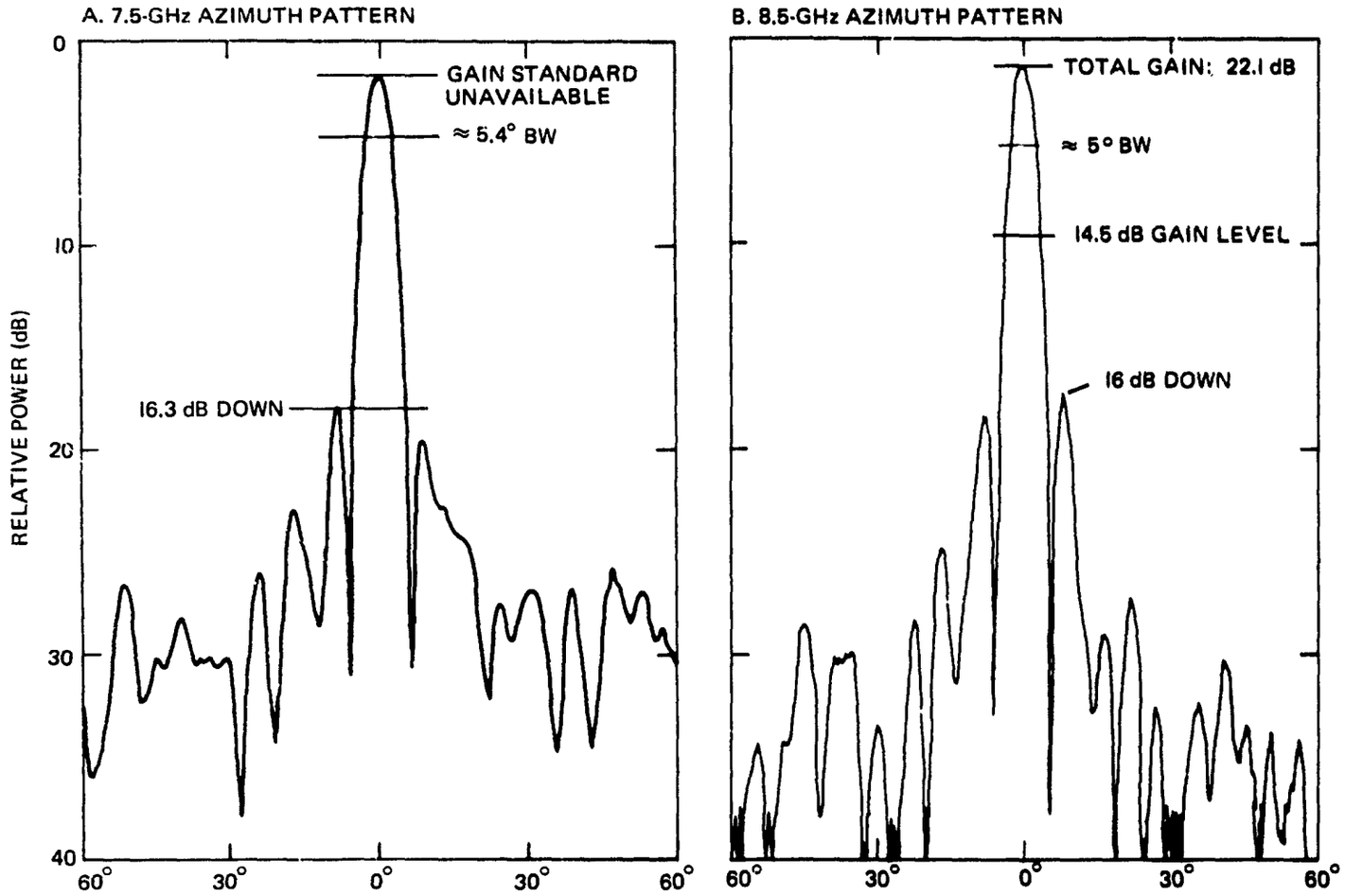

Figure 15. Sectoral feed and source vertically polarized for 18-inch lens at 0° elevation.

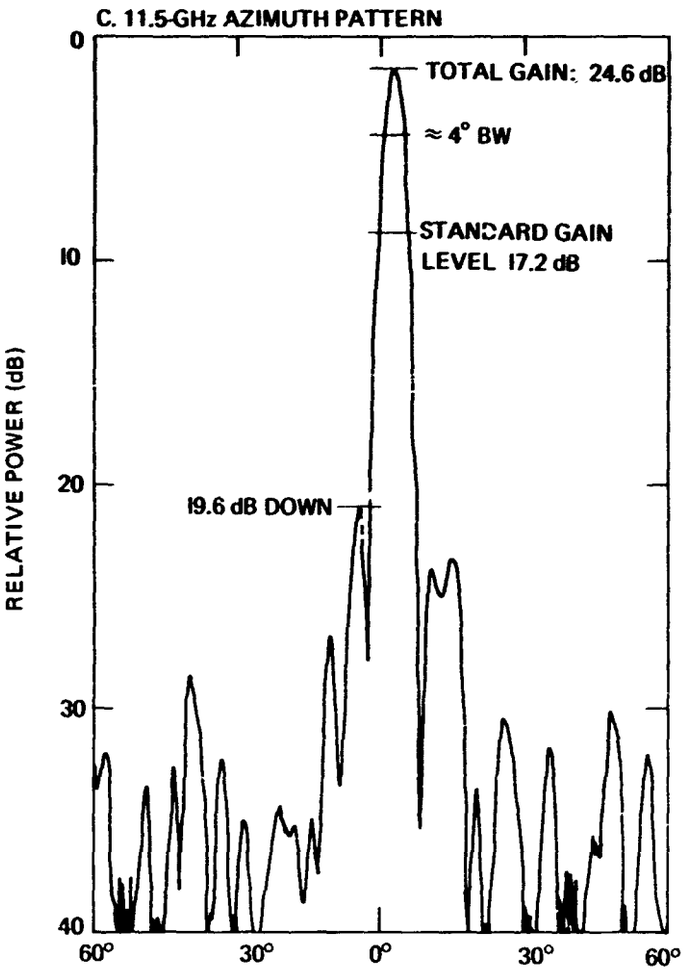

Figure 15. (Continued).

Collectively, these data support the following general conclusions:

1. A lens feed-horn system can be built with fairly uniform gains, beamwidths, and sidelobe response over the 8.5 to 10 GHz-frequency range (over a given 120° sector of the lens).

2. The best focal position should be ascertained, through experimentation, as that which optimizes the gain, beamwidth, and sidelobe response for the intended use. The approach followed by Armstrong in selecting the best focal point was to balance the sidelobe response on each side of the main beam without greatly

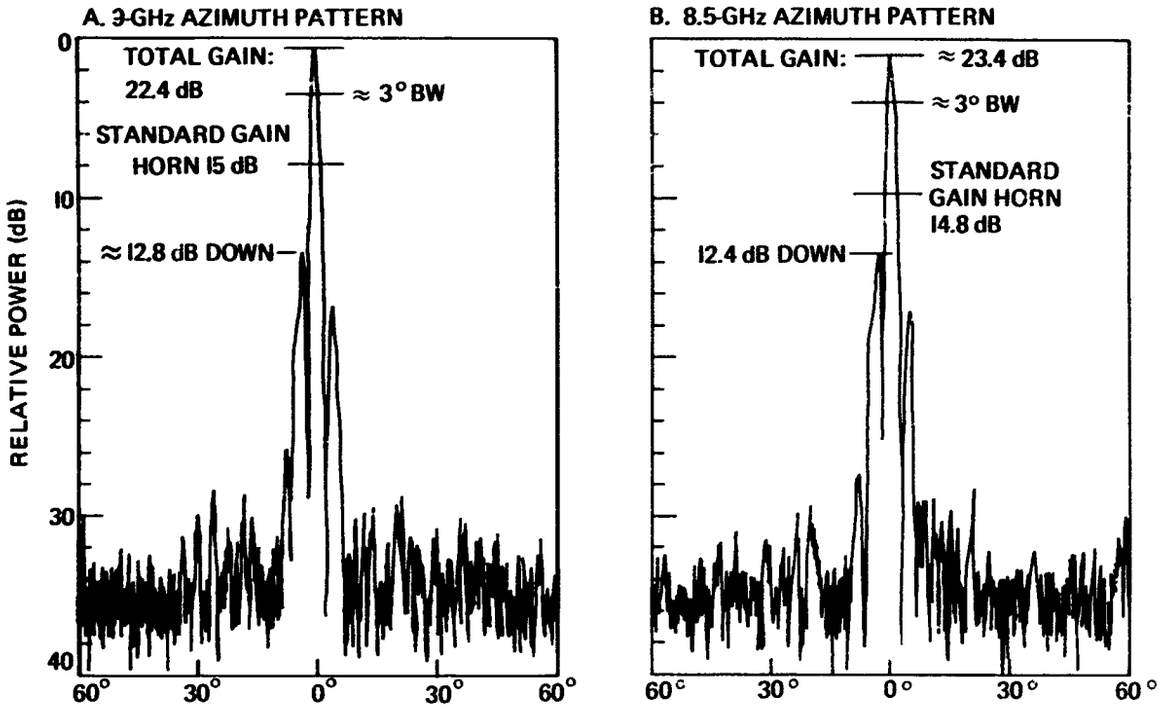

Figure 16. Sectoral feed and source vertically polarized for 44-inch lens at 0° elevation.

reducing the overall gain response. NELC, in general, followed the same practice. However, a number of good beam patterns in the sample data above show a slight imbalance in the first sidelobes.

3. Since the *E*-plane sectoral feed is highly preferential in reception of polarized signals, it makes the lens especially sensitive to the polarization of the source. Later experiments with the 18-inch lens verify this. A spiral feed horn with a small axial ratio was also tested with the 18-inch lens, with good results, against several different linear polarizations.

Composite Patterns for the 18-Inch Lens

After verifying the general suitability of the lens' parameters, the generation of a multibeam pattern, which would indicate the applicability of the lens to a multibeam array, was considered.

Attempts were first made using seven sectoral feeds canted at 45° on 12° centers around the lens (figs. 17-18). These patterns indicated higher gain for horizontal polarization at the selected focal point, some imbalance in gain among the beams, and a general widening of the beams. (All feeds were set at the same focal point.) It was hoped that

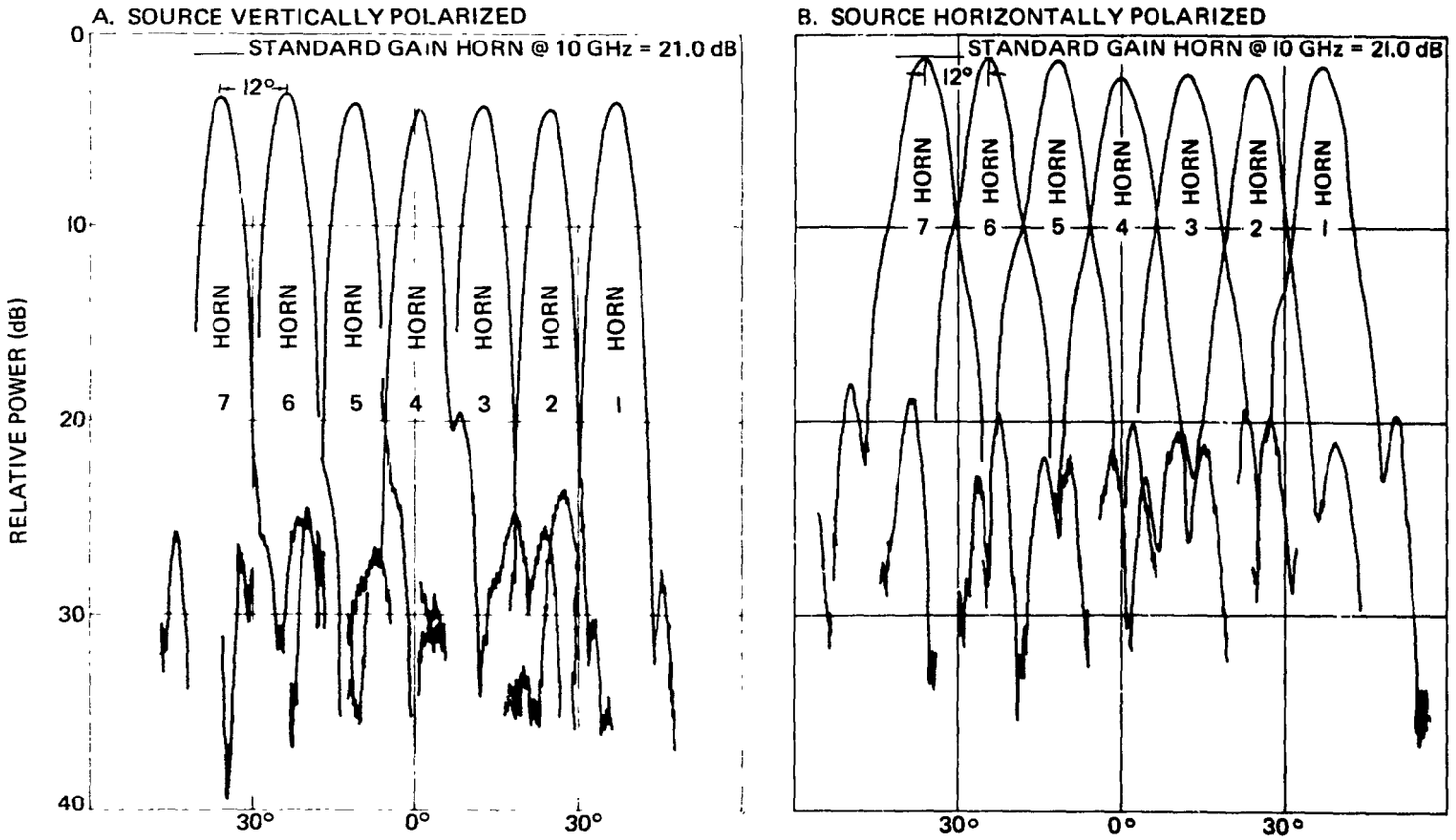

Figure 17. Azimuth patterns at 10 GHz for 18-inch lens with feeds 45° polarized.

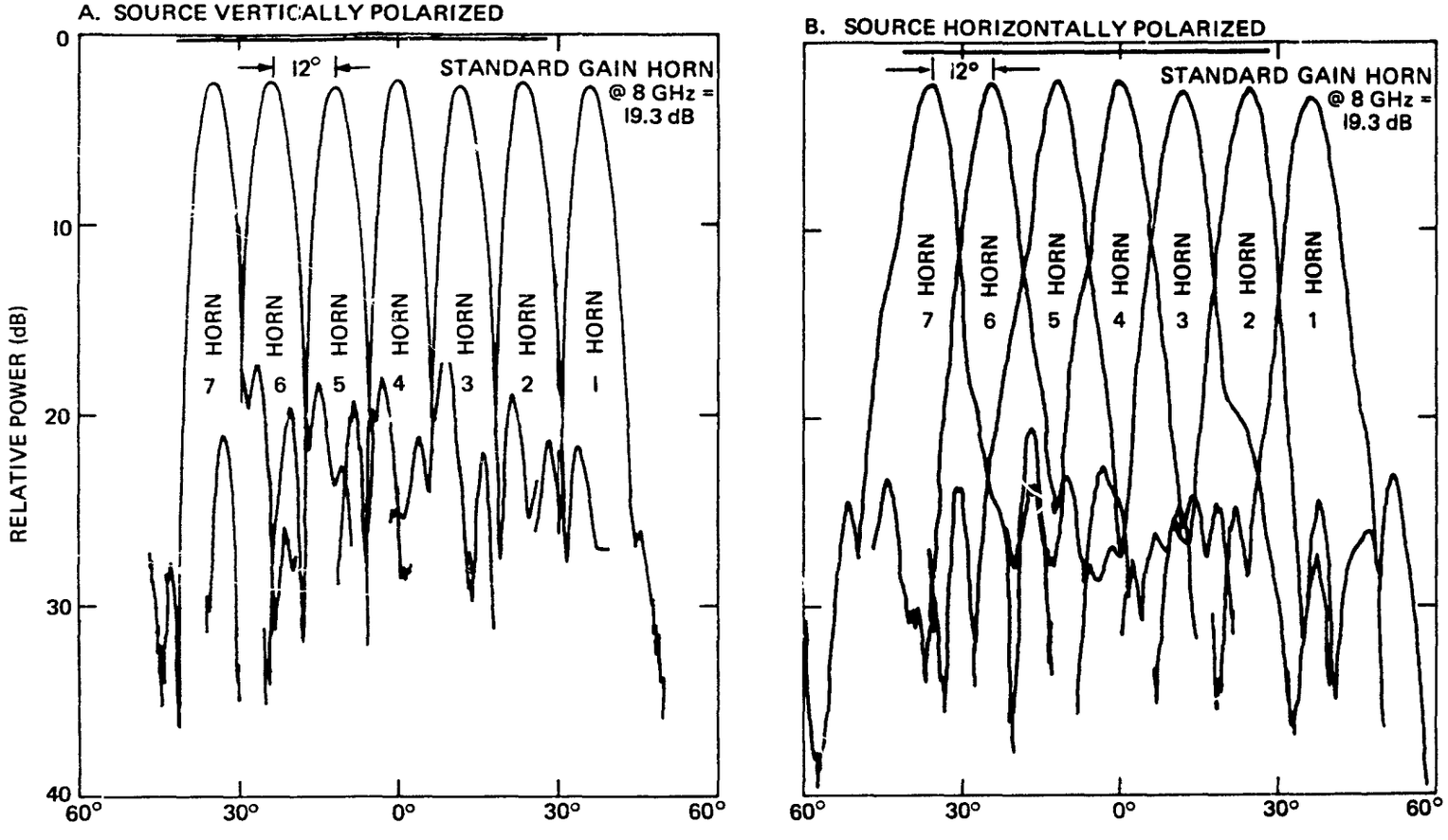

Figure 18. Azimuth patterns at 8 GHz for 18-inch lens with feeds 45° polarized.

canting the feed at 45° would equalize the total gain to vertical and horizontal polarization, but this was not the case. Hence, it appears that the focal point of each feed must be selected independently when gain is imbalanced.

Patterns in figures 19 and 20 give some idea of frequency and azimuth response of individual feeds over a wide azimuth coverage with the other six feeds in place. Main-beam shape is good and is similar to the comparative patterns of the 44- and 18-inch lenses which used a single feed optimized for vertical polarization. Had these, or the composite patterns, shown evidence of serious disturbance of any main beam or excessive side or backlobing, beam interaction would have been blamed and the causes investigated. As it was, all other beams were more or less uniform with the examples shown for horn 1. The wide azimuth patterns, however, showed an increase in sidelobe levels around 120°. This increase was correlated with direct illumination of the feed by the source, indicating a need for shielding the feed horns, at the sides and rear, from direct radiation. (Shielding is discussed in Appendix A.)

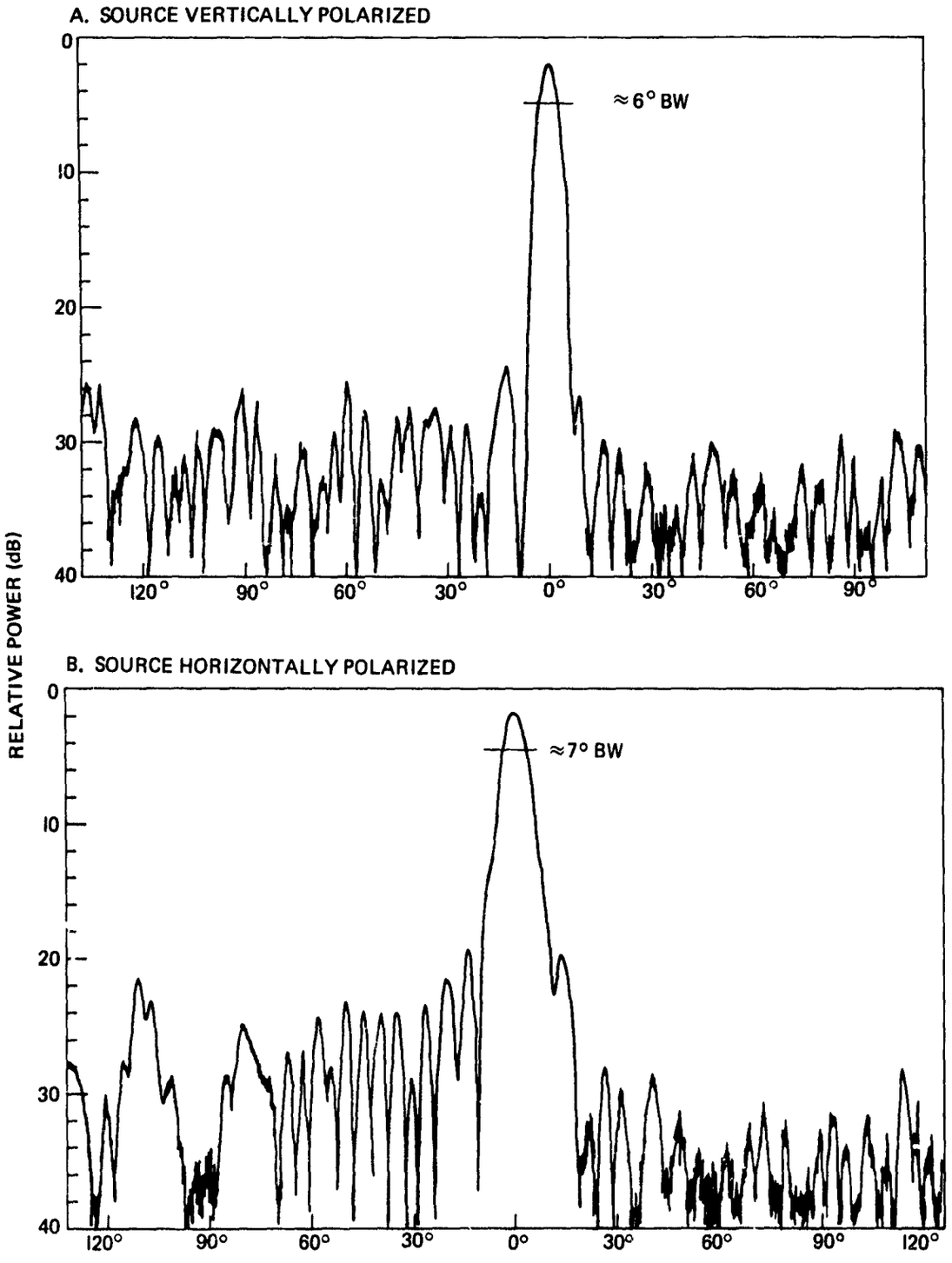

Figure 19. Azimuth patterns at 10 GHz for 18-inch lens with horn 1 canted 45°.

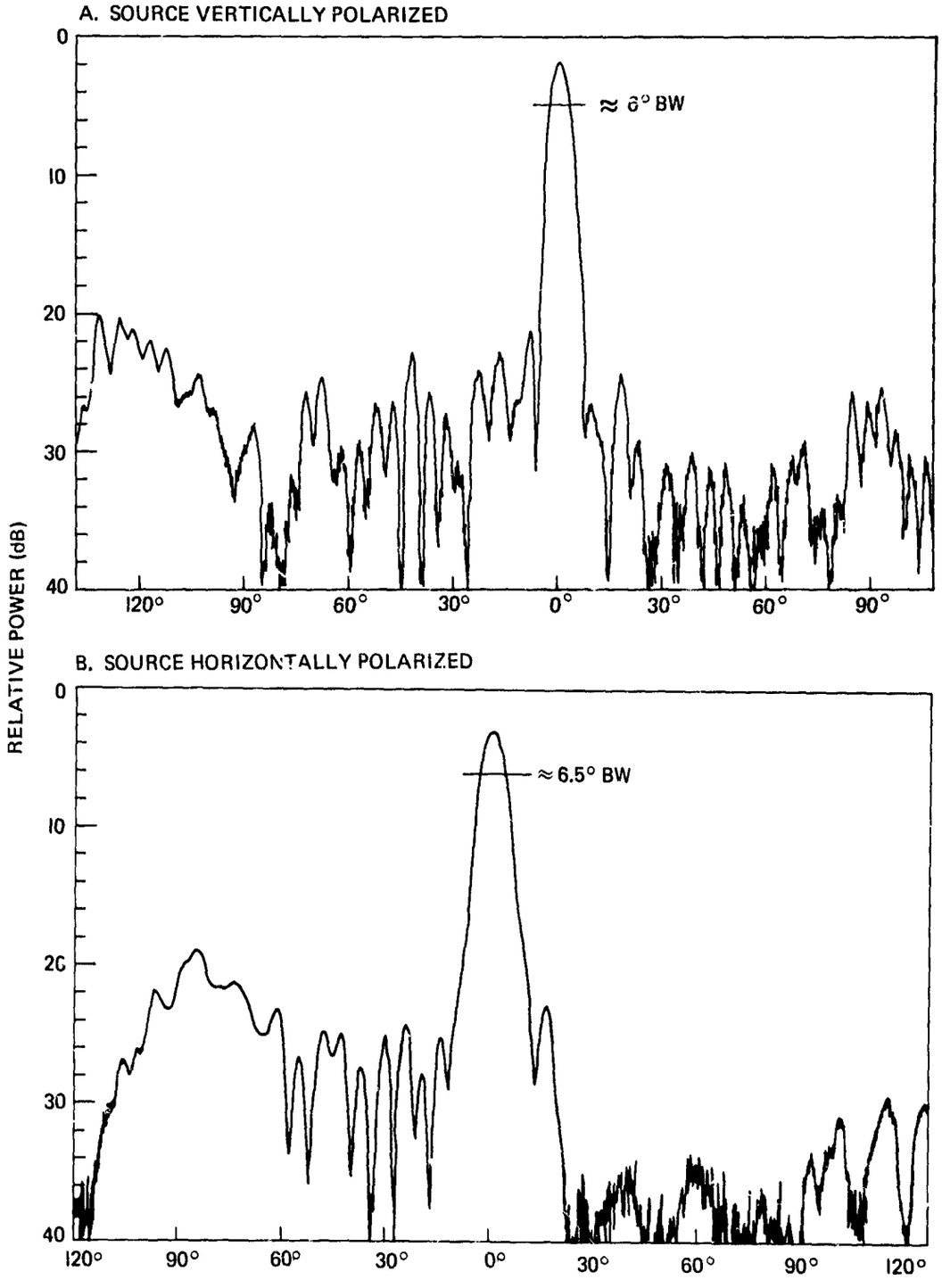

Figure 20. Azimuth patterns at 8 GHz for 18-inch lens with horn 1 canted 45°

Polarization Response of the 18-Inch Lens

The combined response of the lens and feed to various polarizations at 9 GHz is shown in figure 21. Part C shows that the lens-sectoral-feed combination is not equally receptive to all polarizations. When the feed is canted at 45° from vertical, the response of the lens and feed is almost equal, as expected, for either horizontally- or vertically-polarized sources. However, the response to sources polarized 45° left and right of vertical for the canted-feed position did not conform to the expected pattern. It was believed that the lens' response to the 45° polarization of the source, matching the canted feed's position, would be much stronger than its response to the opposite 45° polarization. This would cause the feed and source to be cross polarized. However, this did not occur, and the 45° cross-polarizing signal was transmitted only 8 dB lower than the "matching" 45° signal.

While running the patterns, care was exercised to keep the transmitted power constant. Alignment of the source for the various linear polarizations was crude but close enough so the disparity between the expected and obtained results cannot, in its entirety, be attributed to poor alignment.

Similar polarization measurements using a spiral feed were later run (fig. 22). Like the sectoral feed, the gain response for the spiral is nearly equal for horizontal and vertical polarizations. Also, the beamwidth is greater for horizontally-polarized signals. However, with the sectoral feed, the response to 45° polarization of the source is only slightly less than for vertical and horizontal. Thus the azimuth patterns of the spiral feed indicate a more uniform response to polarized signals than the sectoral feed. On this basis alone, the spiral feed should prove to be the more useful feed to use in implementing a lens-antenna system.

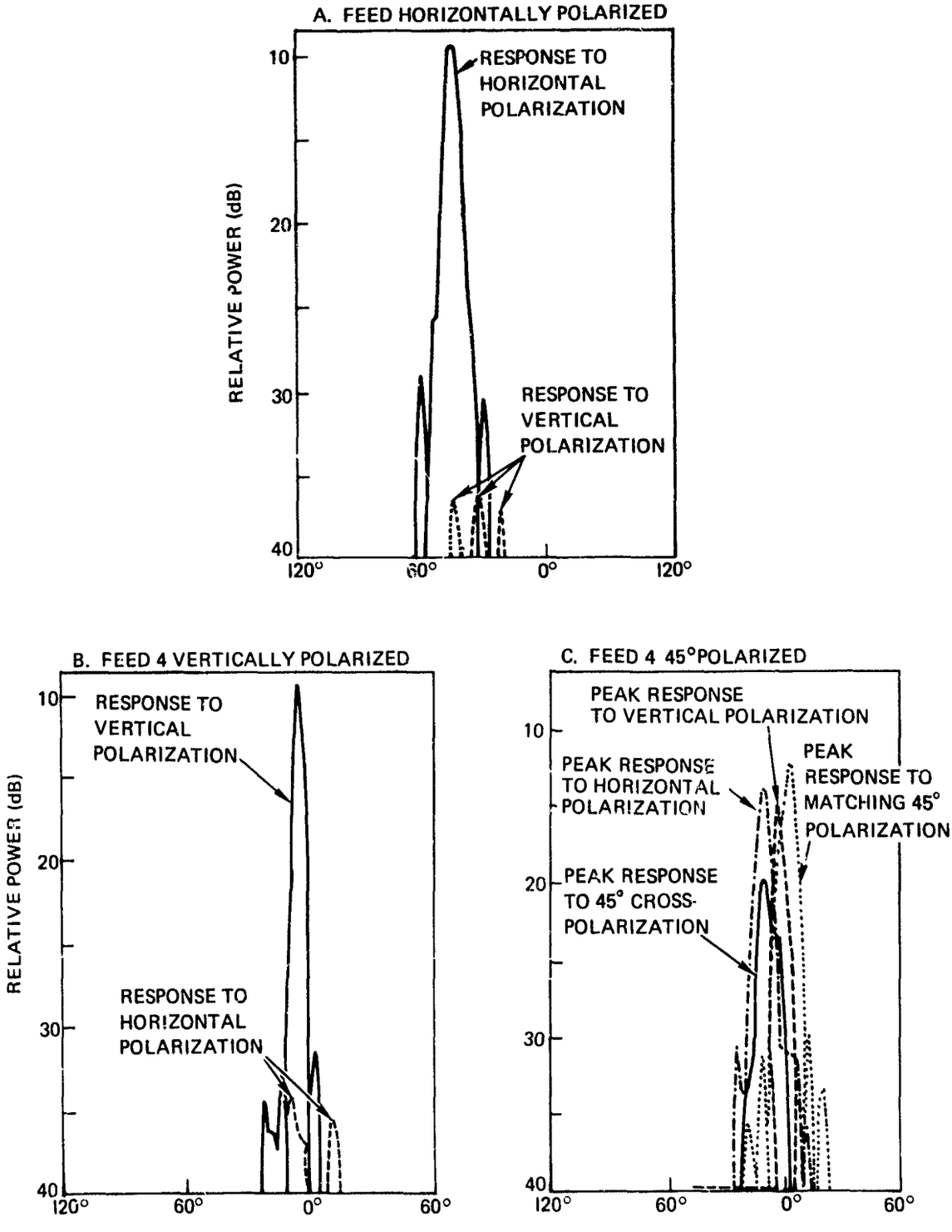

Figure 21 Azimuth patterns at 9 GHz for 18-inch lens with seven horns, 9° separation.

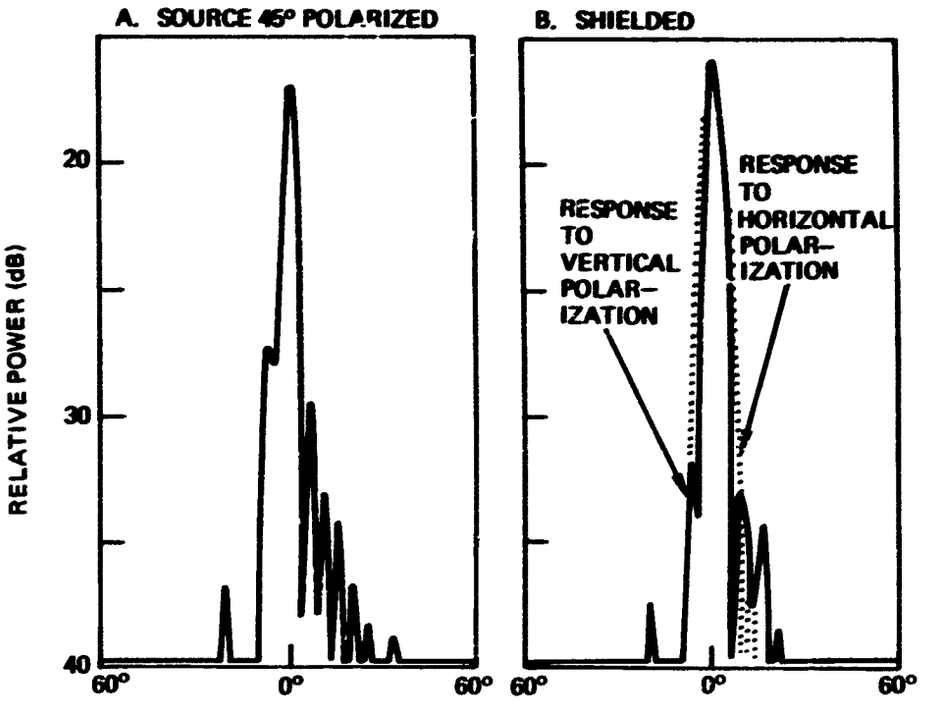

Figure 22. Azimuth patterns at 9 GHz for 18-inch lens with spiral feed (AEL Spiral ASiv 1226A).

Typical Azimuth Patterns of the Constant-K Lens

The constant-K lens was tested on the outside test range using both the *E*-plane sectoral feed, canted at 45°, and the spiral feed. Typical response patterns are shown in figure 23. These patterns can be compared with those of the 18-inch Luneberg lens. For each lens, the gain at 10 GHz is around 18 dB, and the sidelobes are about 20 dB down; however, the constant-K lens has a wider beamwidth (7°) than the 18-inch Luneberg lens (5°).

These patterns were run with the feed horns approximately 8.4 inches from the lens. This is about two times farther from the surface of the lens than predicted by the thick lens formula and about 4.24 times farther out than predicted by the empirical formula of Luoma and Cheston.[3] This extra circumference at the extended focus permitted close spacing of the feeds and, as a result, composite patterns with a very low null depth between adjacent beams. This was verified by using two feeds separated by 5° (fig. 24). The null depth, about 2 dB down, was better than that obtained with the Luneberg. With both channels balanced for gain, it appears null depths approaching 1.5 dB can be expected. This would be a significant step toward achieving uniform response with azimuth. In other respects (gain, sidelobes), the constant-K lens compared favorably to the composite patterns of the 18-inch lens.

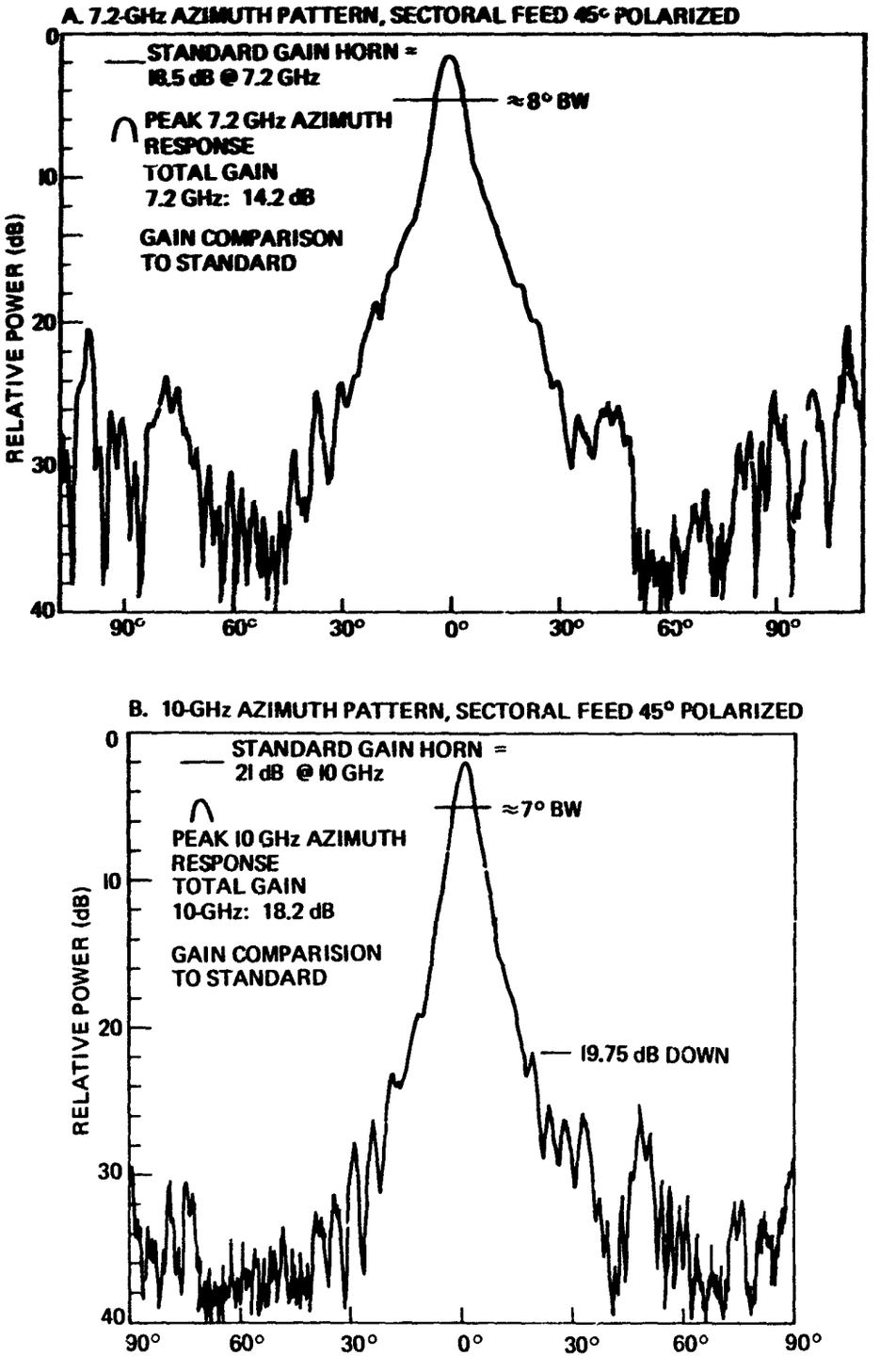

Figure 23. Constant-K lens with source vertically poiarized.

C. 10-GHz AZIMUTH PATTERN, SECTORAL FEED 45° POLARIZED, SHIELDED NEAR MAIN BEAM

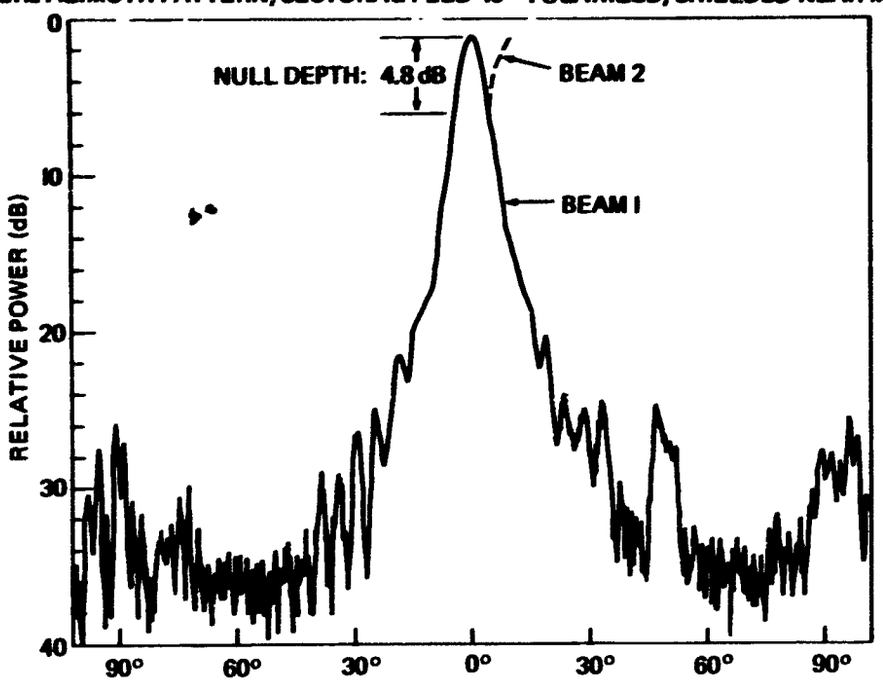

D. 9-GHz AZIMUTH PATTERN, SPIRAL FEED

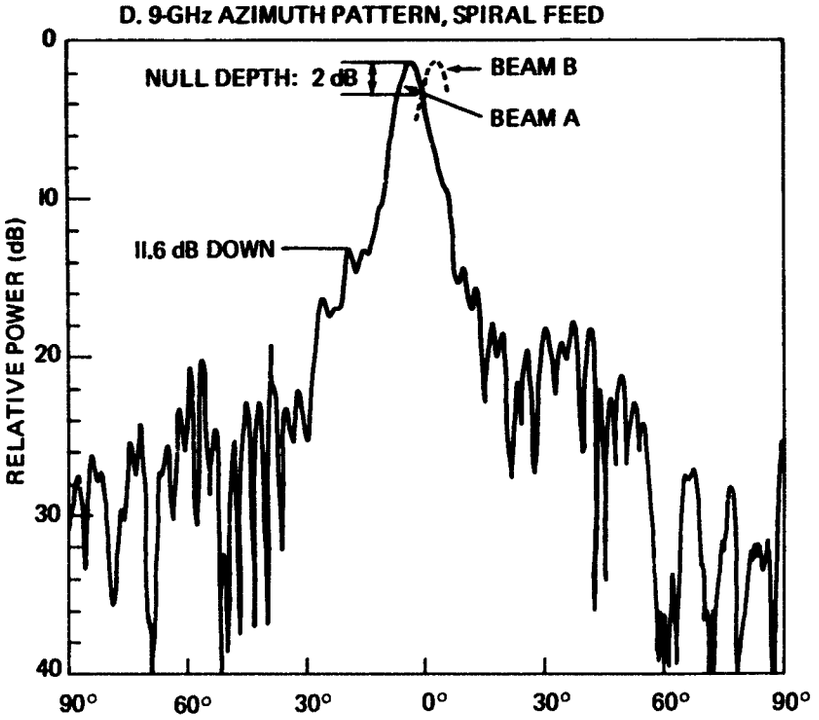

Figure 23. (Continued).

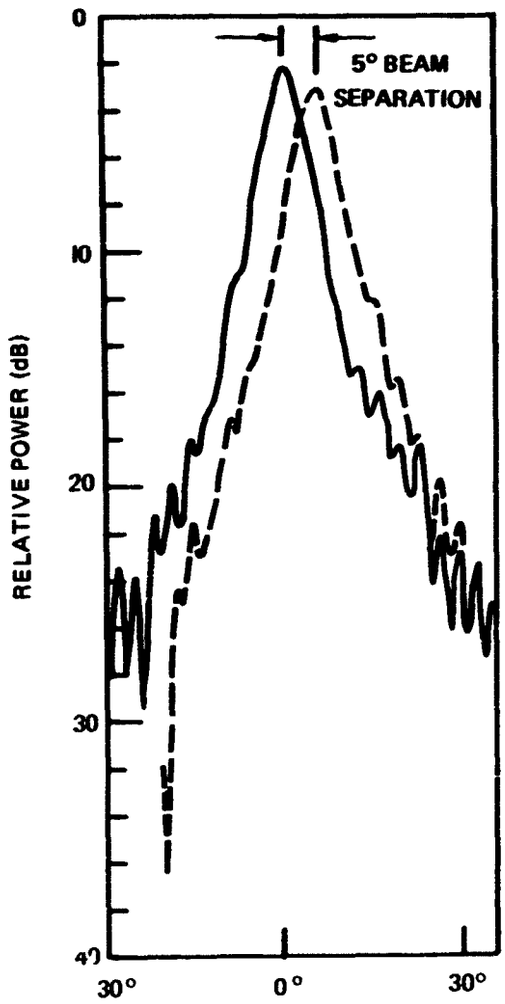

Figure 24. Constant-K lens at 9-GHz azimuth pattern with source vertically polarized, two sectoral feeds, shielded.

It also became apparent tht the extended focus made the feed vulnerable to direct radiation from the source over a very wide azimuth. (This was experienced with the 18-inch Luneberg as the source moved more than 120° off boresight with the feed and lens.) The microwave absorber was used in another test to shield the lens. This time, however, the conducting plates were configured to facilitate adequate placement of the absorber (fig. 25). Despite the absorber, the sidelobes were still high, indicating that special attention must be given to the design of a shield for any serious implementation of the constant-K lens.

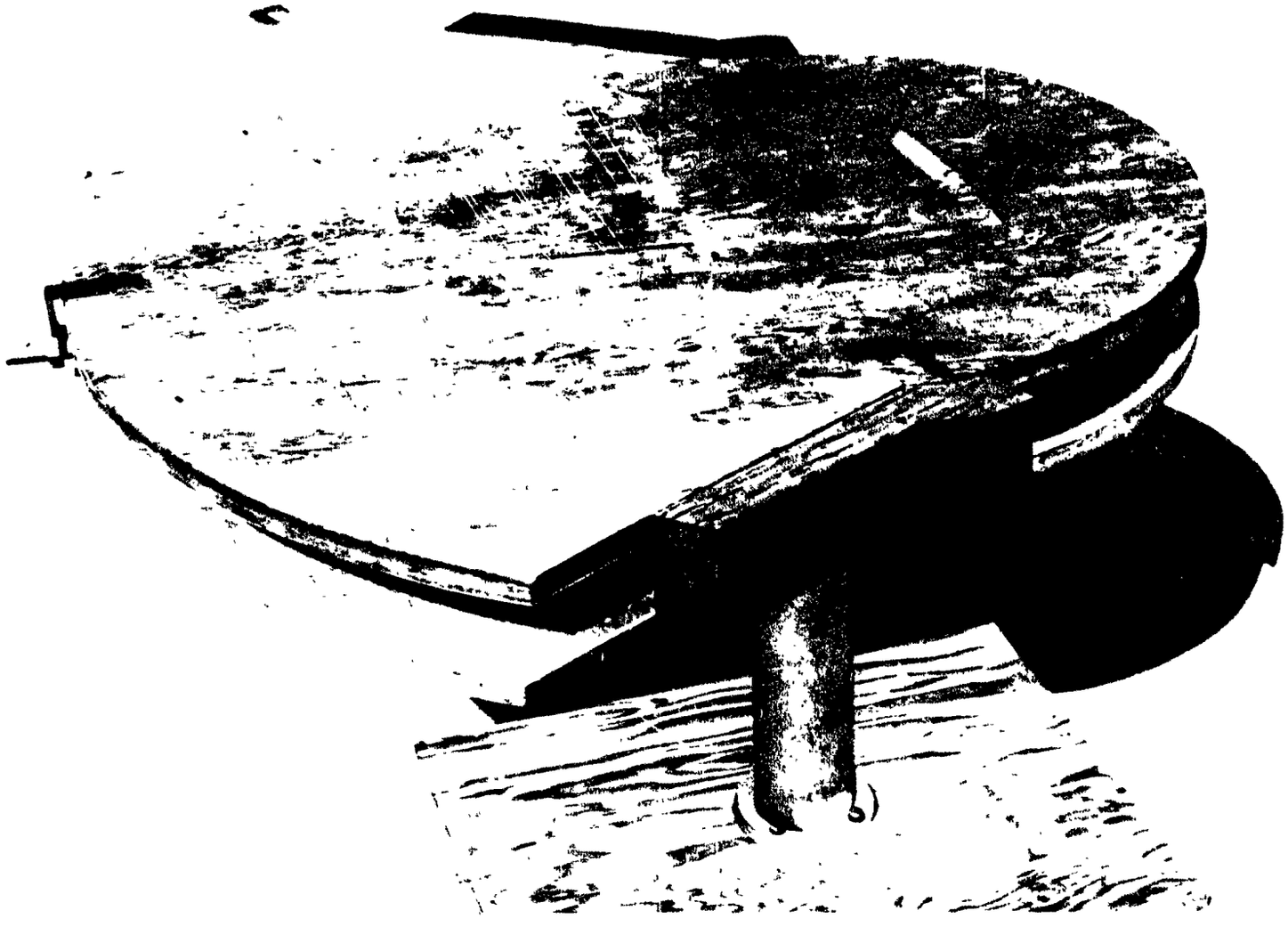

Figure 25. Constant-K lens.

PROPOSED ECM APPLICATION

General Scheme and Objectives

Tests with the Luneberg lens showed that it possesses certain characteristics that can be useful in building a multibeam-antenna array. The test system (Appendix B), while demonstrating these characteristics also introduced some of the problems inherent in implementing such an array in a receiving system. This experience provided the basis for extrapolation to a more practical lens DF receiver and stimulated interest in effective ways of using a lens system for ECM.

Since a lens system has the potential for pulse-by-pulse determination of bearing, it is proposed that it be combined with the IFM receiver, which can determine frequency pulse-by-pulse [5] This combination would permit implementation of an instantaneous broadband frequency-bearing display of emitter activity, which would be more valuable to ECM than either a display of frequency or bearing alone. Also, this approach would provide better frequency resolution and a more compact design for channelizing the frequency band than is possible by combining the lens with contiguous filters.

The proposed combination is illustrated using a single lens in figure 26. However, in a system providing 360° coverage, three lenses would be required, and the IFM antenna would be installed central to the lenses so a pulse incident upon the lens would also be incident upon the IFM antenna. The system would digitally process each pulse and generate a digital or analog voltage proportional to bearing. Simultaneously, the IFM receiver would process its signal data on a pulse-by-pulse basis, and generate either a digital or analog voltage proportional to frequency. These two outputs would then be used to drive a display, showing frequency and bearing.

Whether digital or analog outputs are available, the possibilities for combining the outputs in the display are numerous. The only problem would be equating the relative processing times in the IFM and Luneberg receivers to a common denominator so data pulses could be outputted properly, in the right time frame, to the display.

In addition to providing frequency data to the display, the omnichannel would set a threshold level for comparison with all the directional channels of the lens. Only those directional channels exceeding the omnilevel would be outputted to the Bearing Center Detection Logic (BCDL). The BCDL would select the center or boresight bearing of the directional channels as the bearing to the source.

This technique, like the test system, would operate on a pulse-by-pulse basis. However, it would be simpler and potentially more reliable, requiring fewer thresholds. By means of the variable omnithreshold, the number of directional channels fed to the BCDL would be restricted to a small number, usually three. Since many channels may be energized simultaneously by a single pulse, use of the omnichannel would reduce the logic required in the BCDL which processes the data from the directional channels in parallel. The accuracy of the proposed system using the sidelobe rejection technique would be similar to that of the test system – plus or minus 4.5° or half the distance between adjacent

beam centers. If greater accuracy is desired, secondary comparison of samples from the energized channels, those exceeding the omnichannel can be performed to interpolate among the beams. Suitable "weighting factors" and interpolation among beams should permit accuracies to 1° - 2° without greatly changing the hardware of the previous figure or greatly increasing data-processing time.

There would be a need for overall control of the sample-and-hold-and-compare sequence. This would be handled by the BCDL upon being triggered (alerted) by the breaking of thresholds in either the omnichannel or the directional channels. After the alert, the BCDL would generate sample-and-hold-and-compare, and read triggers in the proper time sequence.

The lens-IFM combination would provide instantaneous coverage over a whole frequency band, *i.e.*, 7-11 GHz, without tuning by the operator. In addition, it would be simple to calibrate and test. To calibrate the lens system, a small probe, fed by a test oscillator, could be inserted into the center of each lens without greatly changing the operation with respect to incident rf waves. The probe would then radiate the test signal into the feed horns around the lens. The same test signal could be also inserted into the input wave guide of the IFM. Calibration and test procedures for the IFM are in NELC Report 1462.[5]

Components of the Proposed System

IFM RECEIVER

The IFM receiver provides the operator with a picture of the entire frequency band being monitored (7-11 GHz), based on an established IFM technique. IFM receivers, already used by the British, have been made in this country by the Syracuse Research Corporation and the Stanford Electronic Laboratories.

The phase difference between signals at the ends of two unequal lengths of transmission line is proportional to frequency. When the sine and cosine outputs of the discriminator are applied to the plates of a CRT, the signal is displayed as a radial line whose angular displacement is proportional to frequency. At *X*-band the tangential sensitivity of a typical unit should approach −70 dBm. (fig. 27).

LENS DIRECTION FINDER (LDF)[6]

Functionally, this unit has been partially defined and the major system aspects shown as in figure 25. However, since it requires fewer multiple thresholds (about two per channel) to cover the complete dynamic range of a crystal detector, it differs from the test system which required at least five thresholds in each channel following a crystal detector. In the test system, individual threshold ranges were small, covering only the decibel range between the crossover nulls and the highest sidelobes from remote beams to prevent interference of sidelobes. (See section on *Composite Patterns*.)

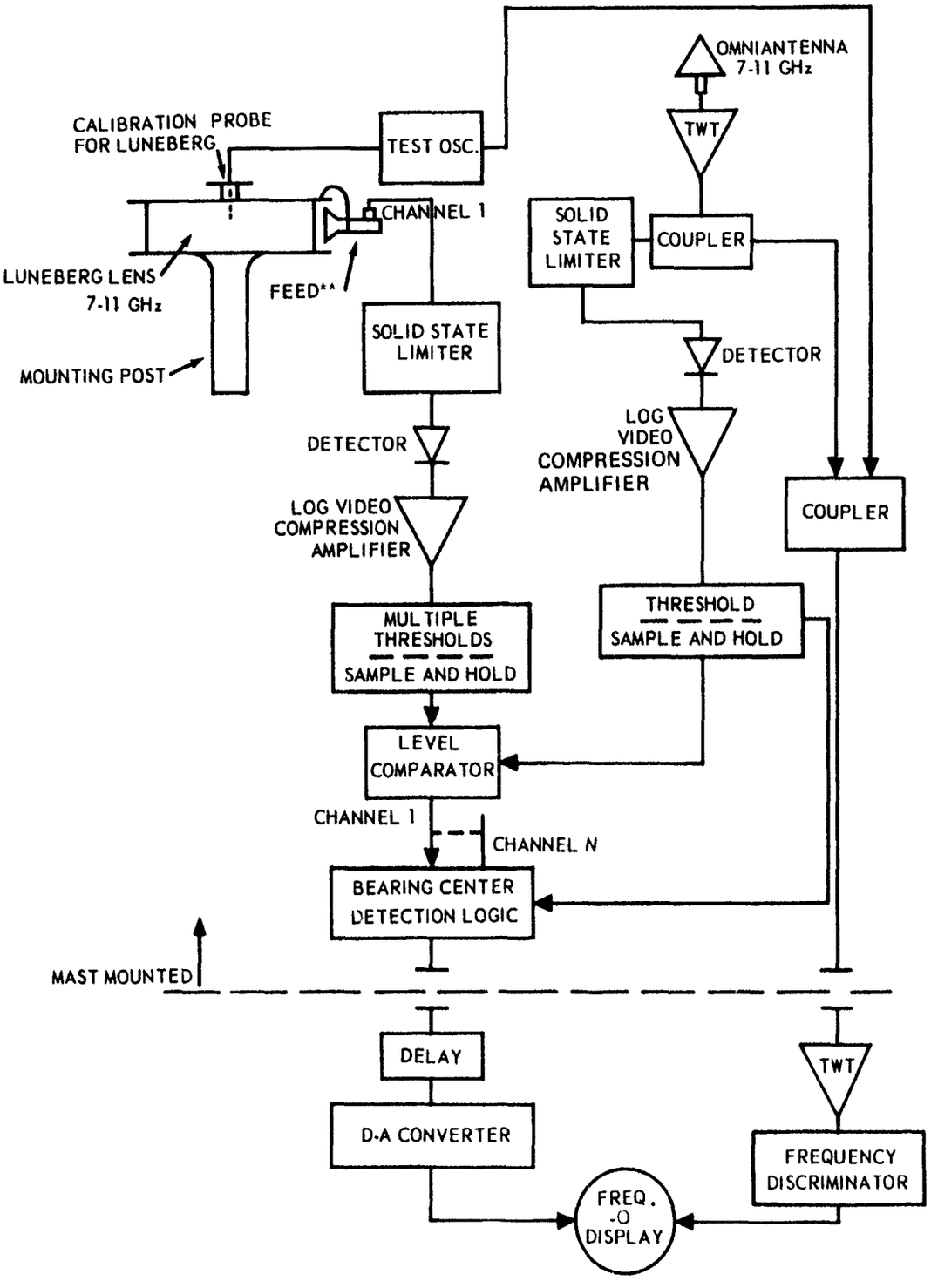

Figure 26. Block diagram of combined Luneberg and IFM receivers.

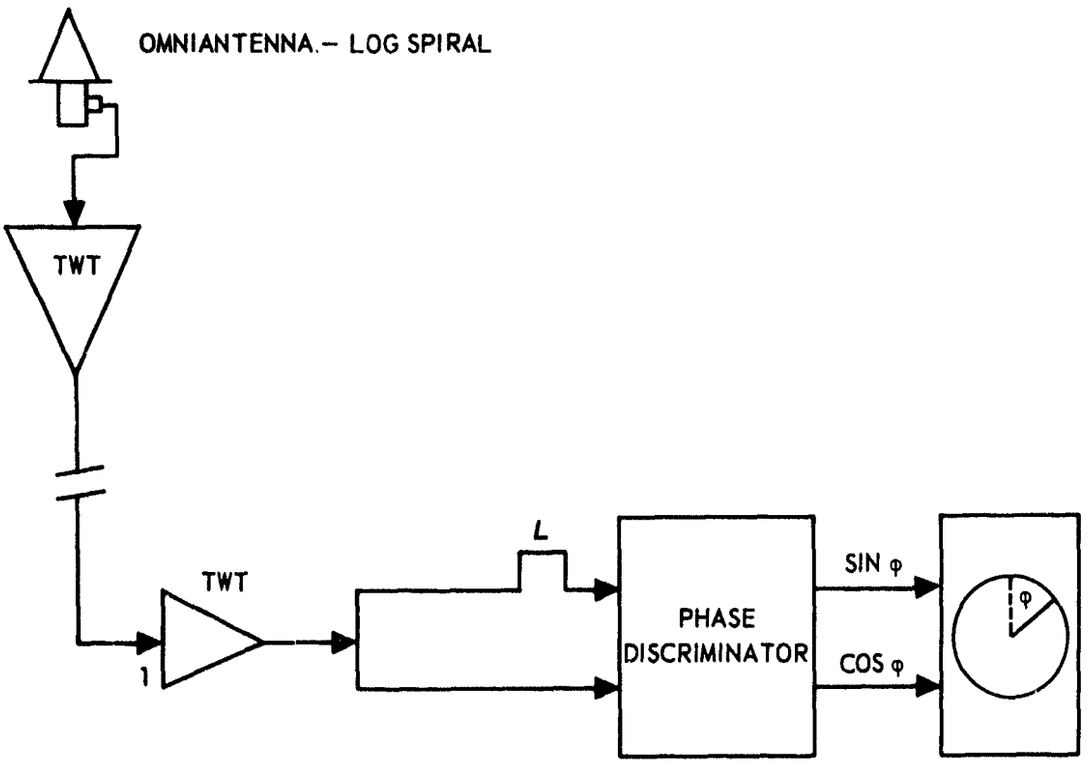

PATH DIFFERENCE = L

PHASE DIFFERENCE, f PHASE DIFFERENCE, $\varphi, = \frac{2\pi L}{\lambda}$

$$= \frac{2\pi L}{C} \cdot f$$

Figure 27. Principle of IFM receiver.

Using the omnichannel in the LDF suppresses sidelobe interference (the omnithreshold level is set higher than the sidelobes) and allows the BCDL to determine bearing based upon main-beam responses only. Thus, individual threshold ranges (only two will be necessary) in each channel can be much wider, and interference from sidelobe or backlobe signals can be suppressed. The thresholds of the directional channels would be required to indicate signals exceeding the minimum discernible signal (MDS), and to pinpoint channels with high level outputs when strong signals are being received. The omnithreshold would further narrow the choice of beams before bearing is determined by BCDL: for example, if eight beams were energized by a signal above MDS and four channels exceeded the second threshold; then these four only would be compared to the omnichannel.

Only those channels exceeding the omnithreshold would be outputted to the BCDL for bearing-center determination. Using the omnithreshold means that either a full DF system with three lenses or a sector-DF-surveillance system (azimuth less than 120°) with a single lens would be possible.

In some cases a sector DF would be desirable. It would lessen hardware requirements and negate the problems of positioning three lenses aboard ship and configuring beams and logic for proper crossover between lenses. The sector DF would still output to a bearing-frequency display similar to a 360° system, but it would be easier to monitor with its narrower azimuth coverage. Also, its smaller number of channels would permit rapid processing of signals. It would thus be suitable for providing limited surveillance and acquistion data, for hand over to fire control or jamming systems. In addition the sector DF could conveniently cover several frequency bands simultaneously: several lenses and feeds could be stacked vertically and matched to the frequency bands of interest. In the sector DF, the antenna for the companion omnichannel would be installed on top of the lenses (fig. 28).

Assuming that only two thresholds are used to cover 40 dB (or 60 dB with the latest crystals), the first threshold would be set slightly above MDS to reduce false alarms, and the start of the second threshold would be about 20 dB above the first. A signal exceeding either would have its "actual" level stored by the sample-and-hold for comparison with the omnithreshold. Since the omnithreshold would be above sidelobe levels, comparison would ensure DF selection based only upon main beams. Consequently, DF accuracy would always be near the maximum attainable.

The video amplifier in each channel would have to permit compression of signals from the detector. Its output, while covering the total dynamic range of the detector, would generate voltage levels compatible with practical sample-and-holds and comparators. However, this would pose no real problem. Nevertheless, the whole design package for the LDF, from solid-state limiters to comparators, is a task calling for a high degree of care in selecting and matching. As a result, consideration should be given to large-scale integration of integrated-circuit technology.

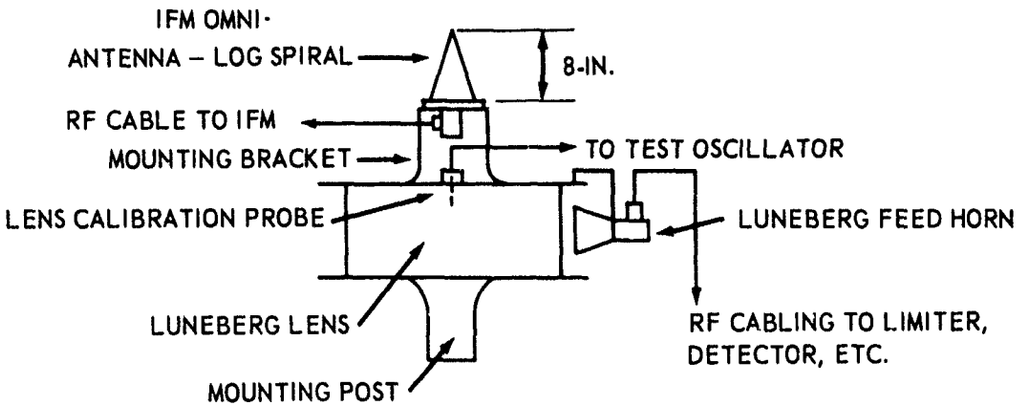

Figure 28. Antenna configuration of sector DF.

DISPLAY

Figure 29 shows a proposed CRT polar display of both bearing and frequency. The bearing storbe (B_1) is generated by deflection voltages from the Luneberg system and is measured clockwise from north, about the actual center of the CRT. The outer end of the bearing strobe (B_1), when stored momentarily becomes the offset-center of the CRT. The frequency strobe (F_1) is generated by deflection voltages from the IFM. It is measured clockwise from north, about the offset-center established by storing B_1.

All incremental bearing strobes between 0° and 360° are of constant radii regardless of signal strength and have their origins at the actual center of the CRT. Their outer-end points sweep out the inner circle which determines the loci of center-offset and bearing for the IFM-frequency strobes. In contrast, the IFM strobes are allowed to vary with signal strength and have their origin, on the circle of center-offset, at the outer end of the coincident bearing pulses from the Luneberg lens.

A suitable bearing graticule and compass-rose can be added to this display to facilitate the reading of bearing and frequency, respectively. A single compass-rose would be required; it should be engineered to permit rotation of its center (anywhere on the center-offset circle) to the origin of frequency strobes of interest (fig. 29). An alternate approach would be a simple Cartesian plot with frequency on one axis and bearing on the other. A dot on the Cartesian plane would indicate a frequency and bearing. A polar plot, in which bearing would be indicated normally as radials and frequency would be marked off in concentric radial bands about the center, could also be considered an approach.

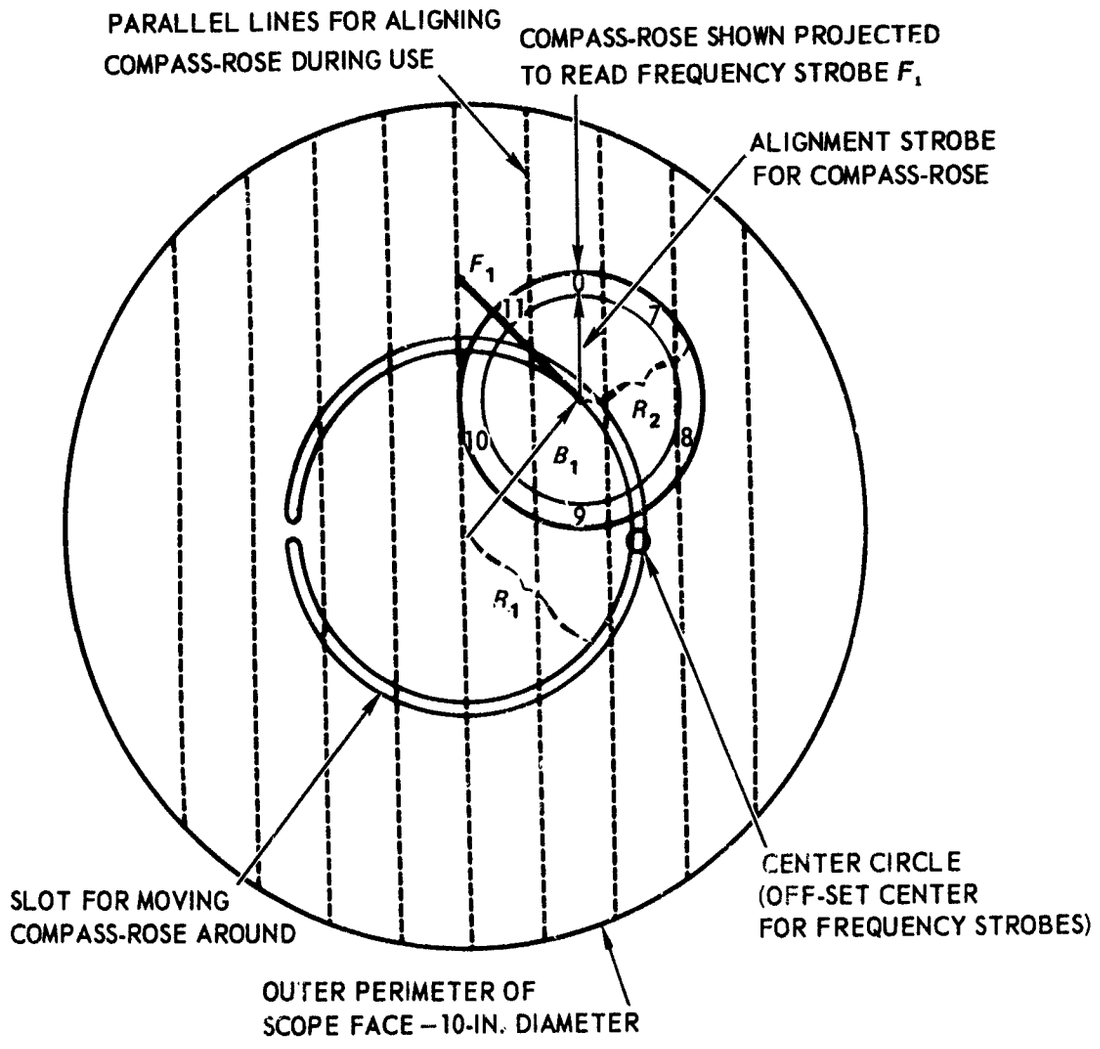

Figure 29. Proposed frequency-bearing display combining outputs from the Luneberg and IFM receivers.

Sensitivity

The threshold sensitivity of the crystal-video channels in the test system was found to be about -40 dBm when thresholds were set to give a moderately low false-alarm rate. This, in conjunction with a lens antenna having a gain of 18 dBm (-1dB), sets the minimum received power at the antenna at -58 dBm (± 1dB). This figure is optimistic and should be degraded by several decibels to reflect rf-cable runs and the lower false alarm rate (higher threshold setting) required in a practical system.

If greater system sensitivity is desired, the wideband crystal-video channels can be replaced by superheterodyne channels but not without an increase in cost per channel.

One method for implementing the superheterodyne channels to give instantaneous rf coverage is to utilize a separate homodyne local-oscillator channel. This involves receiving the rf signal on a separate antenna and mixing it with an internal signal equal to the i-f. The resulting output would be filtered to obtain only the upper or lower sideband frequency, which would be used as the local-oscillator frequency for the superheterodyne channels. A multichannel representation is shown in figure 30.

A second approach involves the use of wideband i-f amplifiers and two banks of solid-state comb-local oscillators, time shared to the mixer, to permit surveillance of the total 7-11-GHz-band for the shortest expected pulsewidths. The comb oscillators would be chosen so that signal components of a single comb would not interact to produce spurious signals at i-f. It is possible to use two or more i-f's per channel, simplifying selection of i-f amplifiers and comb frequencies for instantaneous coverage of the total band.

Using either of the latter two techniques, it is expected that a sensitivity in the low 60's could be obtained. Any discrepancy between lens direction finder (LDF) and the IFM could be balanced by thresholds or attenuators. However, for a given intercept, the two receivers have to be gain matched so the overall gain in the directional channels of the lens is greater than the overall gain of the omnichannel. In practice the omnichannel's gain would be set just above the sidelobe gain of the directional channels.

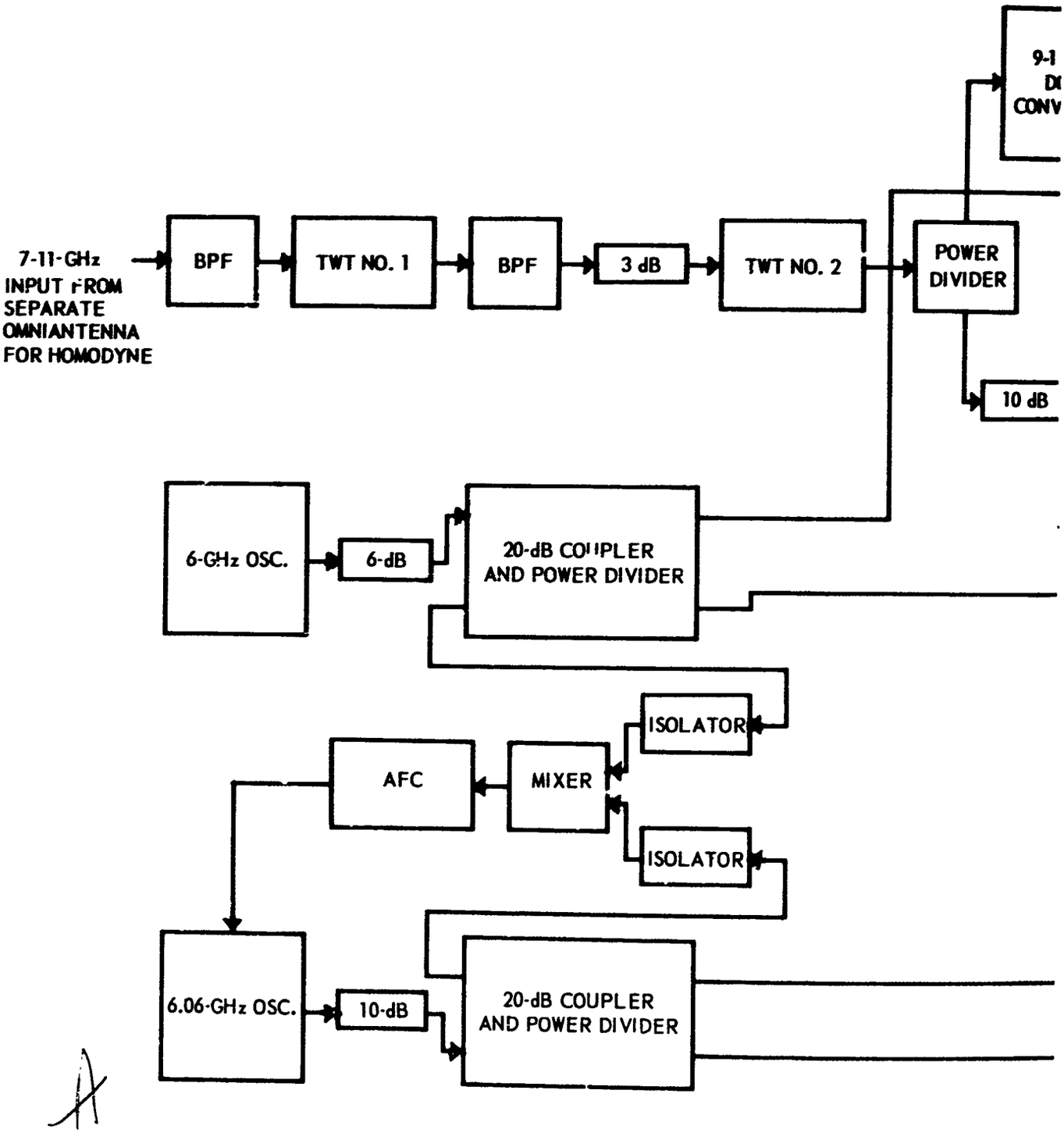

REVERSE SIDE BLANK

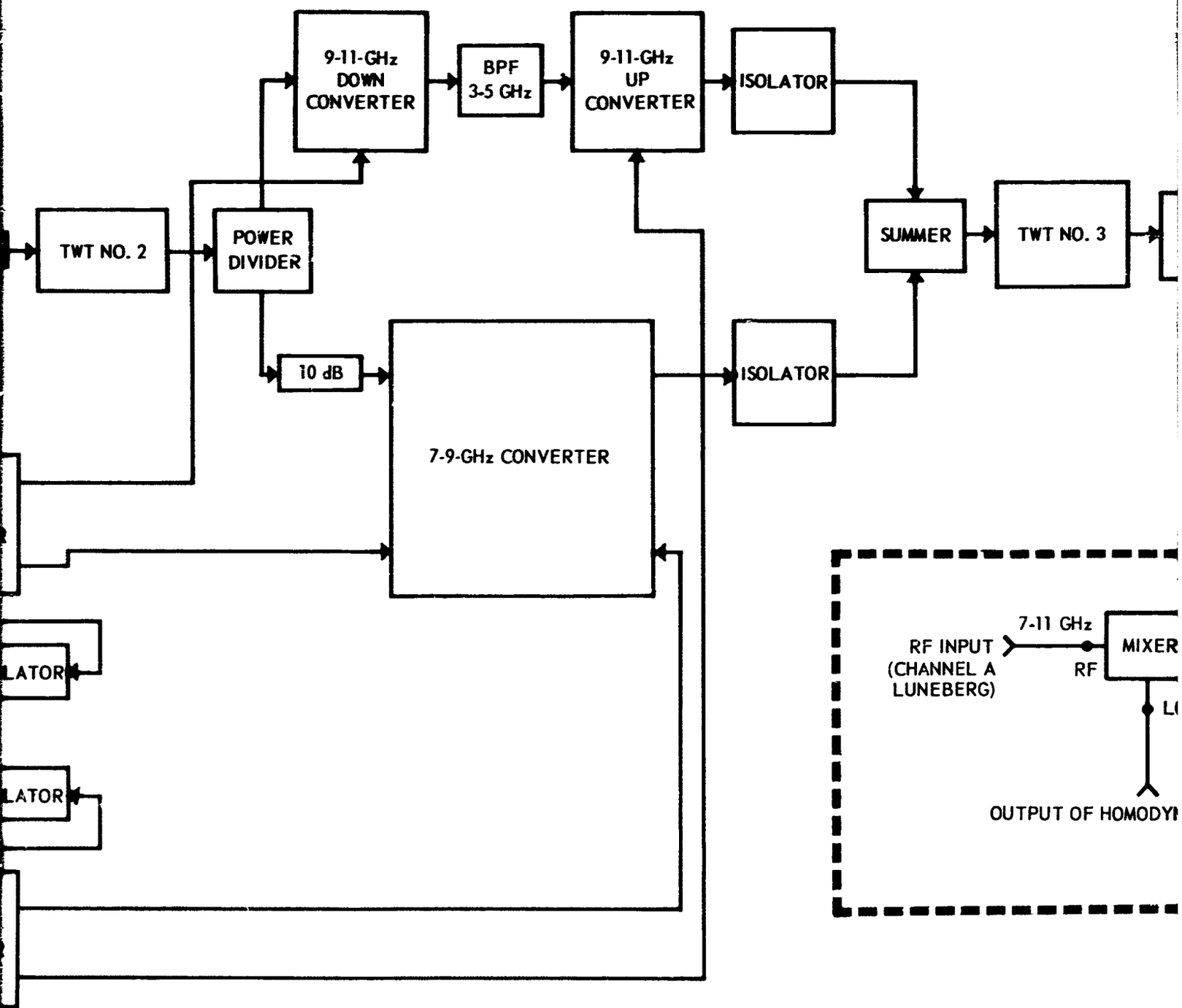

Figure 30 Block diagram of new homodyne local oscillator (input mixer would be divided into N outputs to feed N chann

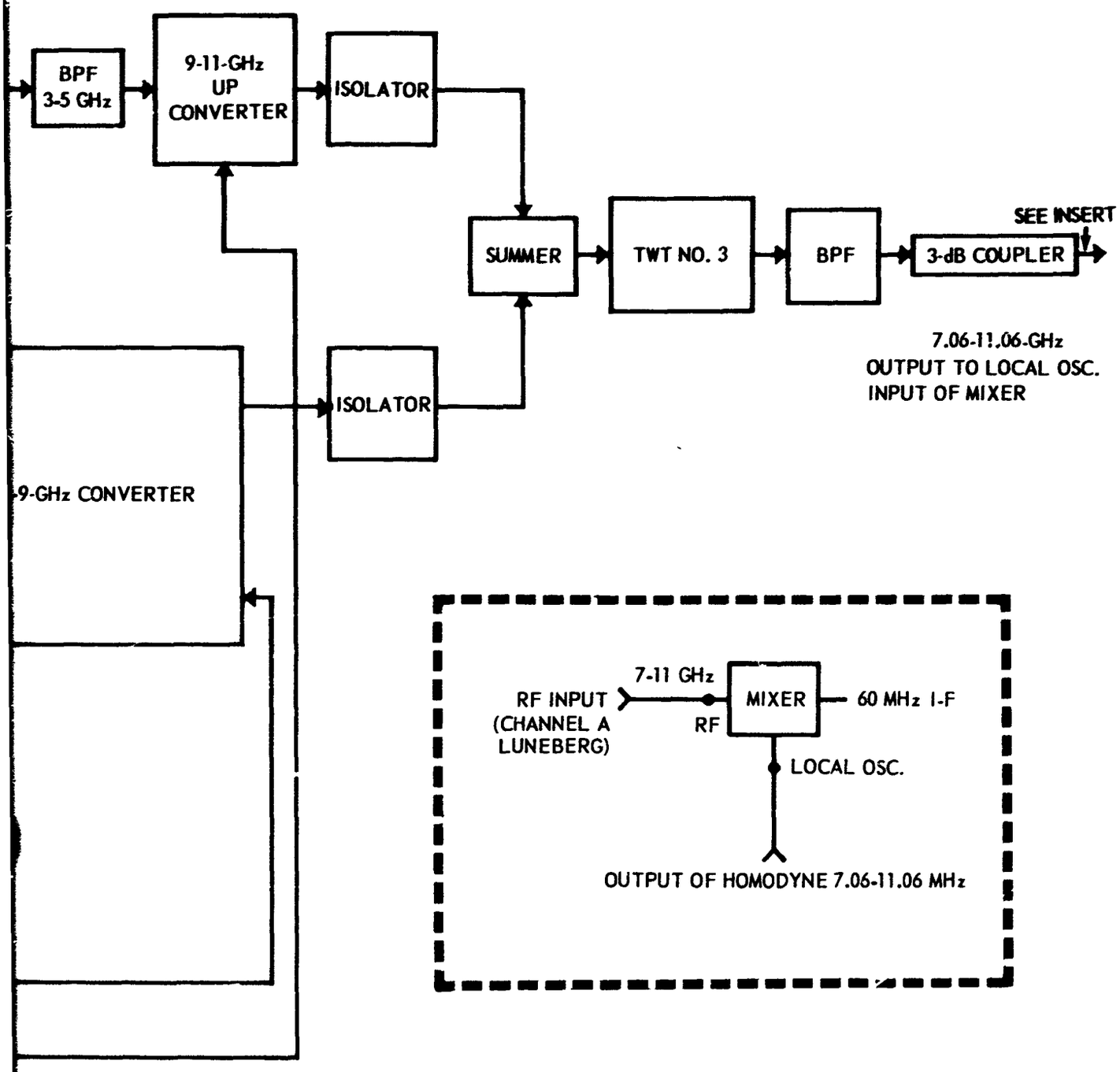

Figure 30. Block diagram of new homodyne local oscillator (input to local-oscillator channel of mixer would be divided into N outputs to feed N channels of the Luneberg system)

CONCLUSIONS

1. Technology exists for manufacturing low-loss, high-gain Luneberg and constant-K lenses for antenna applications over the 7-11 GHz frequency range.

2. With the proper selection of feed horns, the Luneberg or constant-K lens can provide high gain, narrow beamwidths, low sidelobes, and the acceptance of multiple polarization.

3. The multiple-beam patterns of the 18-inch Luneberg lens indicate that it may be implemented as a multibeam direction finder when combined with appropriate receiving and display techniques

RECOMMENDATIONS

1. Use a properly shielded Luneberg lens to generate response patterns of beams which lie at the periphery of the 120° azimuth coverage of a single lens.

2. Generate multibeam patterns for the constant-K lens. (Space feed horns between 5°-9° apart.)

3. Implement and evaluate a lens direction finder using a single Luneberg lens with *E*-plane sectoral feeds and an omniantenna for sidelobe suppression.

REFERENCES

1. Luneberg, R.K., *Mathematical Theory of Optics*, p. 189-213, Brown University Press, 1944

2. Morgan, S.P., "General Solution of Luneberg Lens Problem," *Journal of Applied Physics*, v.29, p. 1358-1368, September 1968

3. Cheston, T.C. and Luoma, E.J., "Constant-K Lenses," *APL Technical Digest (Applied Physics Laboratory)*, v.2, p. 8-11, March-April 1963

4. Buckley, E.F., "Stepped-Index Luneberg Lenses," *Electronic Design*, v.8, p. 86-89, 13 April 1960

5. Navy Electronics Laboratory Report 1462, *NEL Program For a Small-Ship Electronic Warfare System*, by C.V. Tenney and E.R. Billam, CONFIDENTIAL, 1 June 1967

APPENDIX A: SPECIAL AZIMUTH PATTERNS FOR CONTROLLED TESTS – 18-INCH LENS

Microwave Absorber as a Shield

REDUCTION OF SIDELOBES AND BACKLOBES OF AZIMUTH PATTERNS

Tests were conducted with the 18-inch lens in an anechoic chamber to reduce sidelobes and backlobes of azimuth patterns. The use of the chamber permitted interference-free measurements and gave the operators freedom to make polarization adjustments to the source and feeds, thus allowing a number of additional patterns to be run at 9 GHz.

Figure A1 shows the vertical response pattern of the lens and feed 4 when the rear and sides were both shielded and unshielded from direct illumination by microwave-absorbing material. Figure A2 shows the lens with the microwave absorber in place (Figure A3 presents a similar comparison for horn 7.) Obviously, the shield of absorbing material aided in lowering sidelobes by reducing direct illumination of the feeds. This appears to be an advantage in regard to system implementation since the gain differential (dynamic range) between sidelobes and main beams is increased. (Future research efforts should include running similar patterns with a source many times stronger to obtain a fine-grain look at the resulting sidelobes.)

The absorber type-AN74, used in making the shield, is manufactured by Emerson and Cuming, Inc., of Canton, Massachusetts. It is usable for frequencies above 3.5 GHz and provides about 20 dB attentuation. Snug-fitting holes were cut in the absorber to pass over the feeds, and the ends were curled snugly against the lens. Care was exercised in placing the absorber between the feeds so the sides of the feeds' dielectric loading were not covered.

REDUCTION OF THE PROJECTED PLANE APERTURE OF THE LENS

The shield, composed of the microwave absorber, proved to be valuable as a means of reducing sidelobes and backlobes. It also stimulated interest in the use of absorbing material to limit the forward aperture of the lens, *i.e.*, reduction of the projected plane aperture from 18 inches (diameter of the lens material) to a smaller size. The results of tests for feed with the other six feed horns and the shield of the microwave absorber in place, are shown in figure A4. The results show that aperture reduction causes a decrease in gain. It also appears to cause some change in beamshape which, together with gain reduction, is normally expected for a reduced aperture. In figure A4 (A and B) it is evident that the additional absorber aided in reducing sidelobes which were only partially suppressed by the shield. Similar results were obtained for horn 3 (fig. A5).

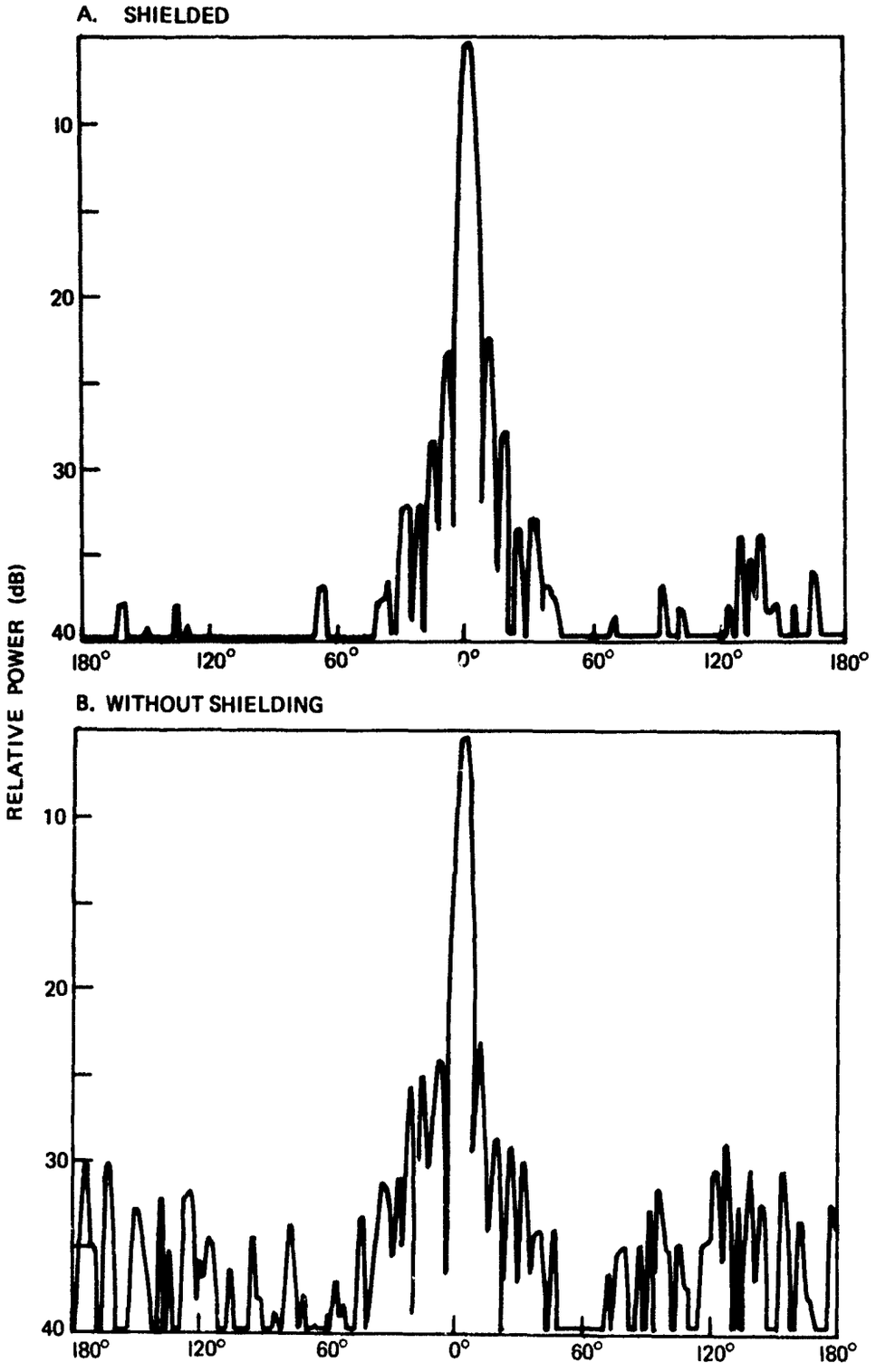

Figure A1. Azimuth patterns at 9 GHz for horn 4 with source vertically polarized, seven horns, and 12° separation.

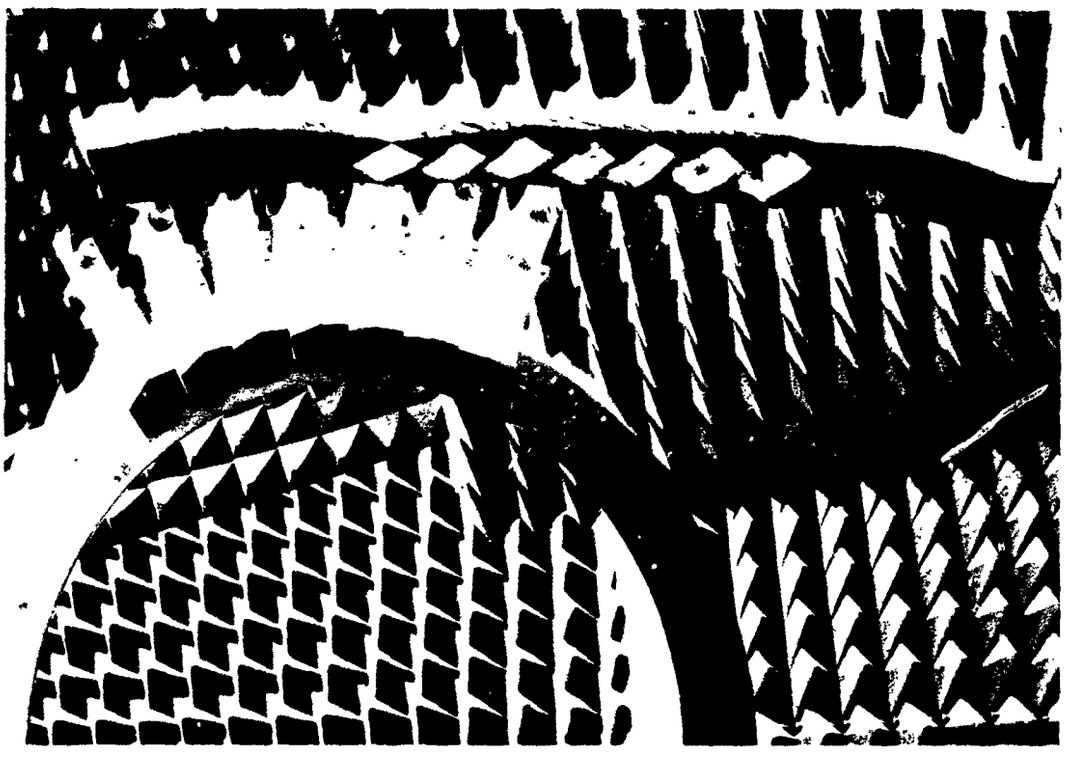

Figure A2. Luneberg-lens mounting for horns showing shield of microwave absorber.

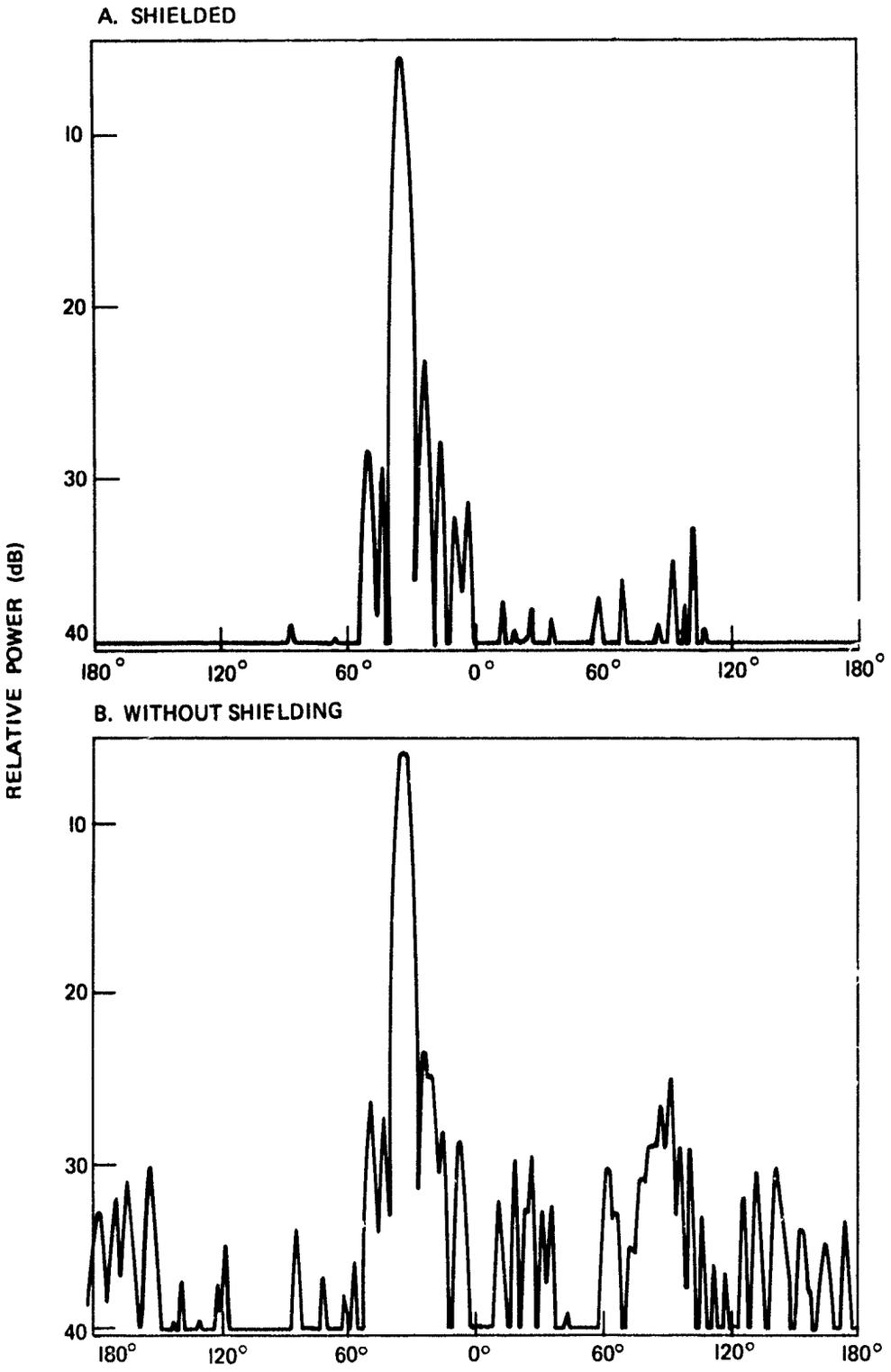

Figure A3 Azimuth patterns at 9 GHz for horn 7 with source vertically polarized, seven horns, and 12° separation.

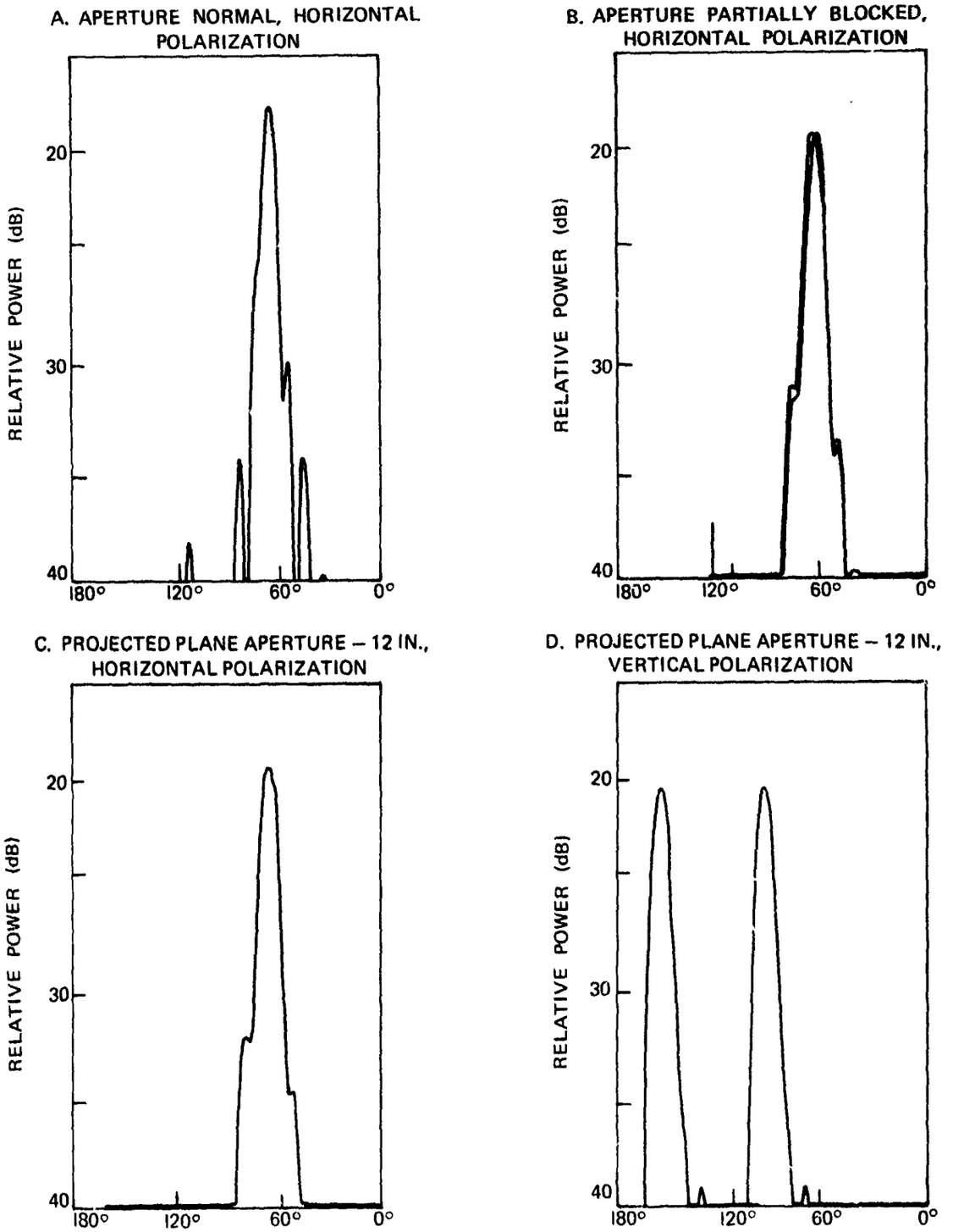

Figure A4. Azimuth patterns at 9 GHz with 18-inch lens for horn 4, unloaded and shielded, with 9° separation

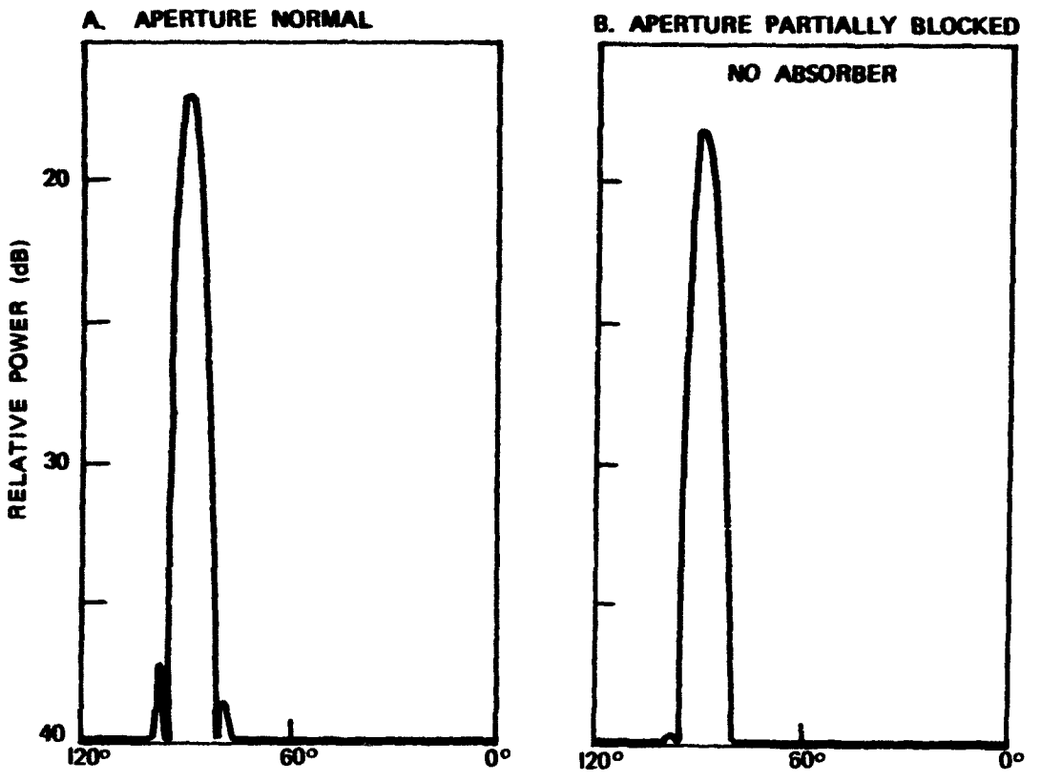

Figure A5. Azimuth patterns at 9 GHz with 18-inch lens for horn 3, loaded and shielded, with vertical polarization and 9° separation.

Effects of Loaded Versus Unloaded Feeds

Figure A6 shows the response pattern to horizontal polarization with and without teflon loading (the lens aperture is not reduced by the absorber). The loaded feed showed higher gain and a reduced sidelobe response. This was expected since the loaded feed, being more directive, rejects more off-center energy from the lens than does the unloaded feed. From this it appears that restricting energy acceptance (or illumination) mainly to a narrow amplitude taper about the center of the lens is a way to reduce sidelobes. These data also seem to validate the idea that horn dimensions could be made smaller (for closer spacing) without jeopardizing apparent aperture if a material of higher K, but similar loss characteristics, is used for loading. This would be essential for Luneberg system applications where beams must be spaced close together to reduce null depth between adjacent beams. The higher K-loading would keep the apparent aperture constant, although the feeds would be made smaller to permit closer spacing. (Figure A7 is included for comparison.)

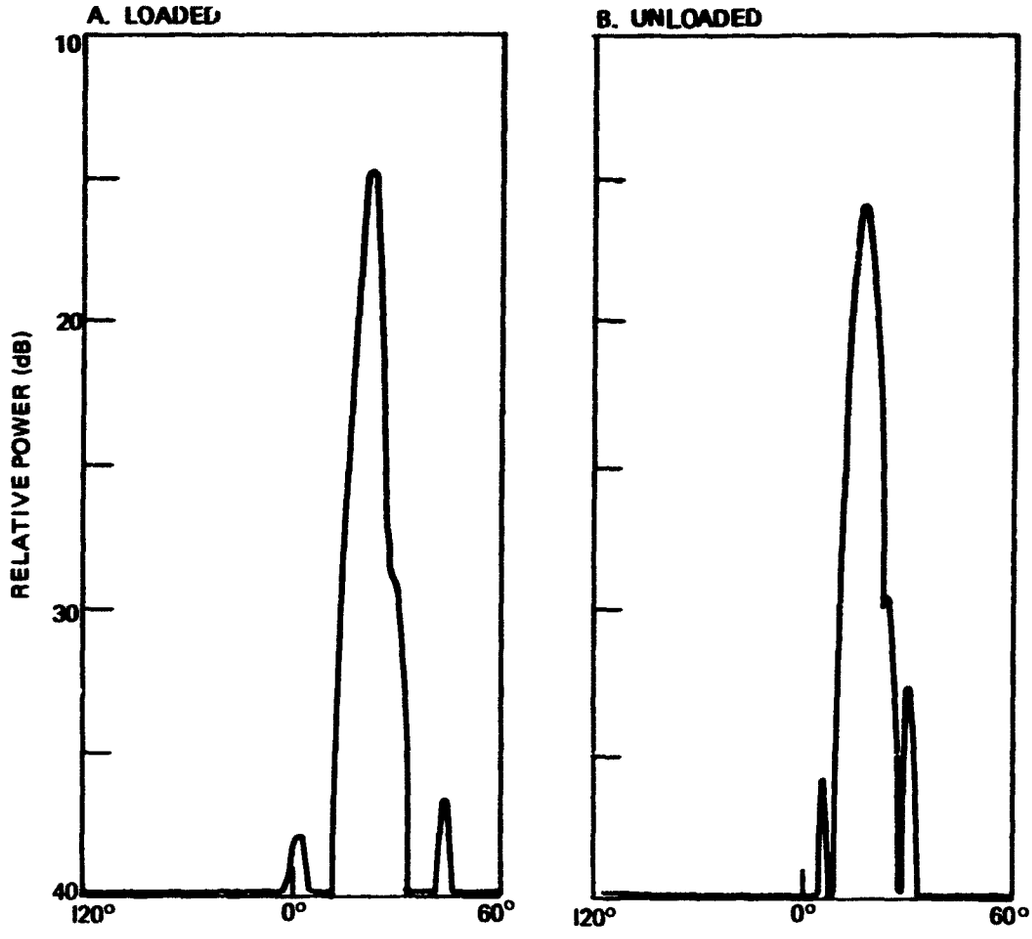

Figure A6. Azimuth patterns at 9 GHz with 18-inch lens for horn 4, shielded with horizontal polarization, 9° separation, and normal aperture.

Effects of Varying the Focal Position of Feeds

The azimuth patterns in figure A4 were run at a different focus for the feeds than were those for figures A5 and A6. The former were at a longer focus, approximately 6/16-inch longer. Figures A4(A) and A6 (B) with horn 4 unloaded at different foci, show a change in beamshape between the two. There is also a gain differential, with the feed at the longer focus (Fig. A6(B) exhibiting the lower gain. Figure A8 shows the same feed at an even closer focus, approximately 6/16-inch closer than for figure A6,(A). Again, a change in beamshape is noticeable. In addition, the sidelobe responses are further removed from the main beam. This latter point may be a significant finding, but it is difficult to draw conclusions on such limited data. Again similar data on the 44-inch lens (fig. A9) are included for comparison.

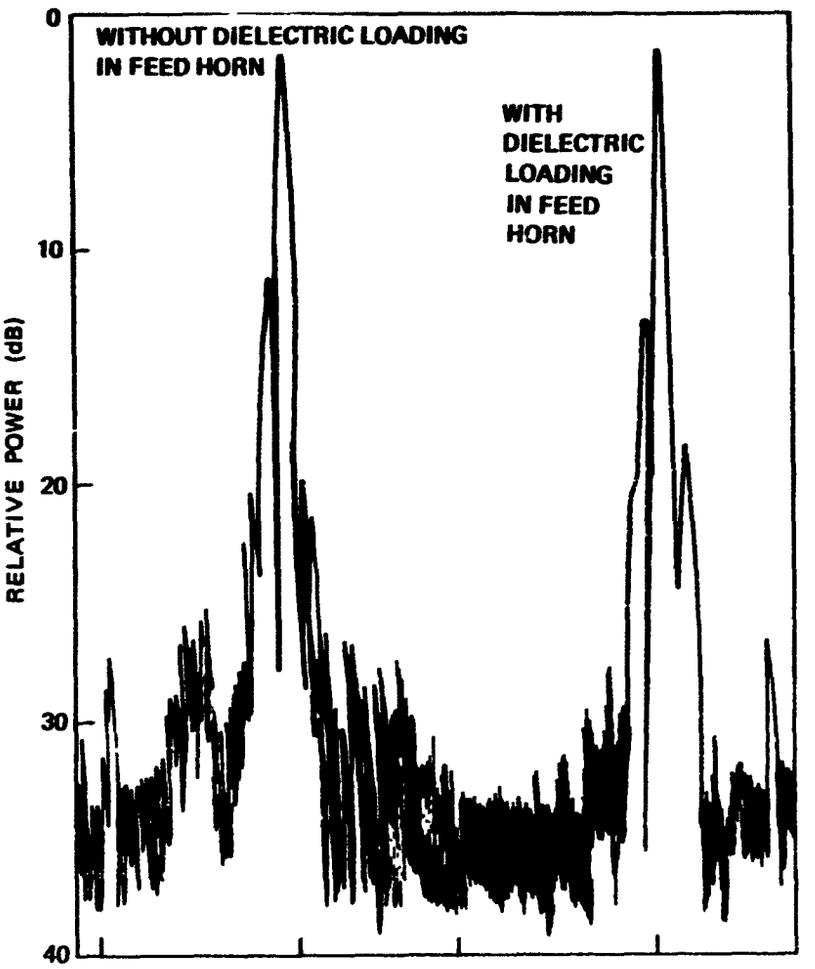

Figure A7. Azimuth patterns at 10 GHz for 44-inch lens with sectoral feed and source vertically polarized and 0° elevation.

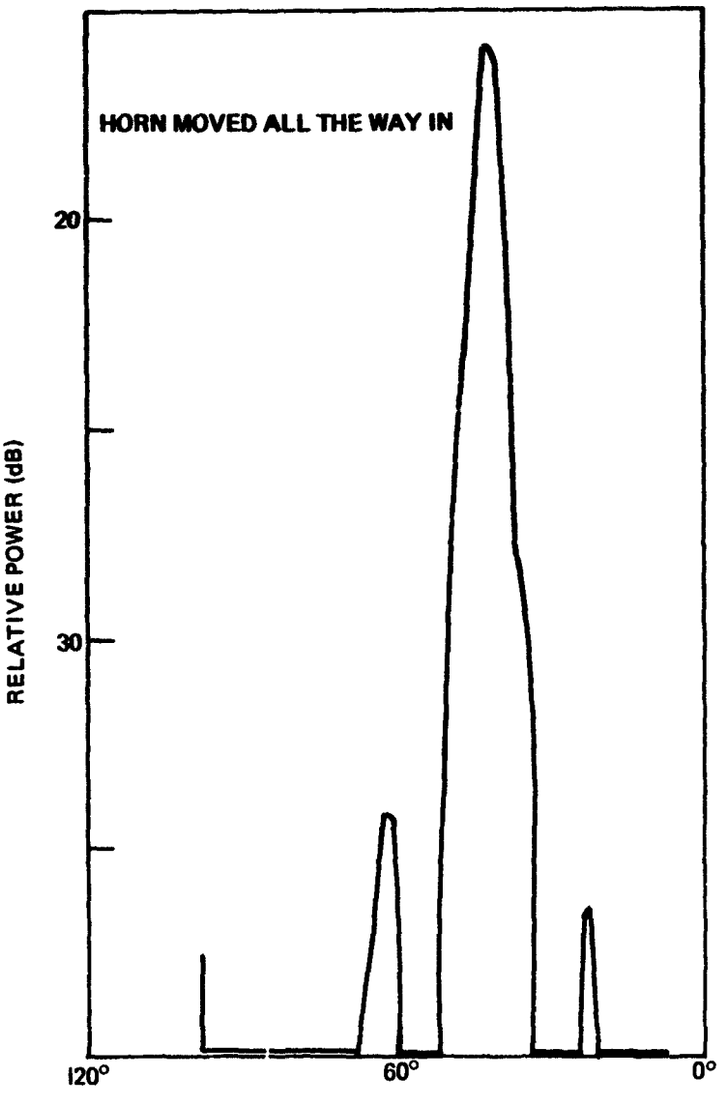

Figure A8. Azimuth patterns at 9 GHz with 18-inch lens for horn 4, unloaded and shielded, with horizontal polarization, 9° separation, and normal aperture.

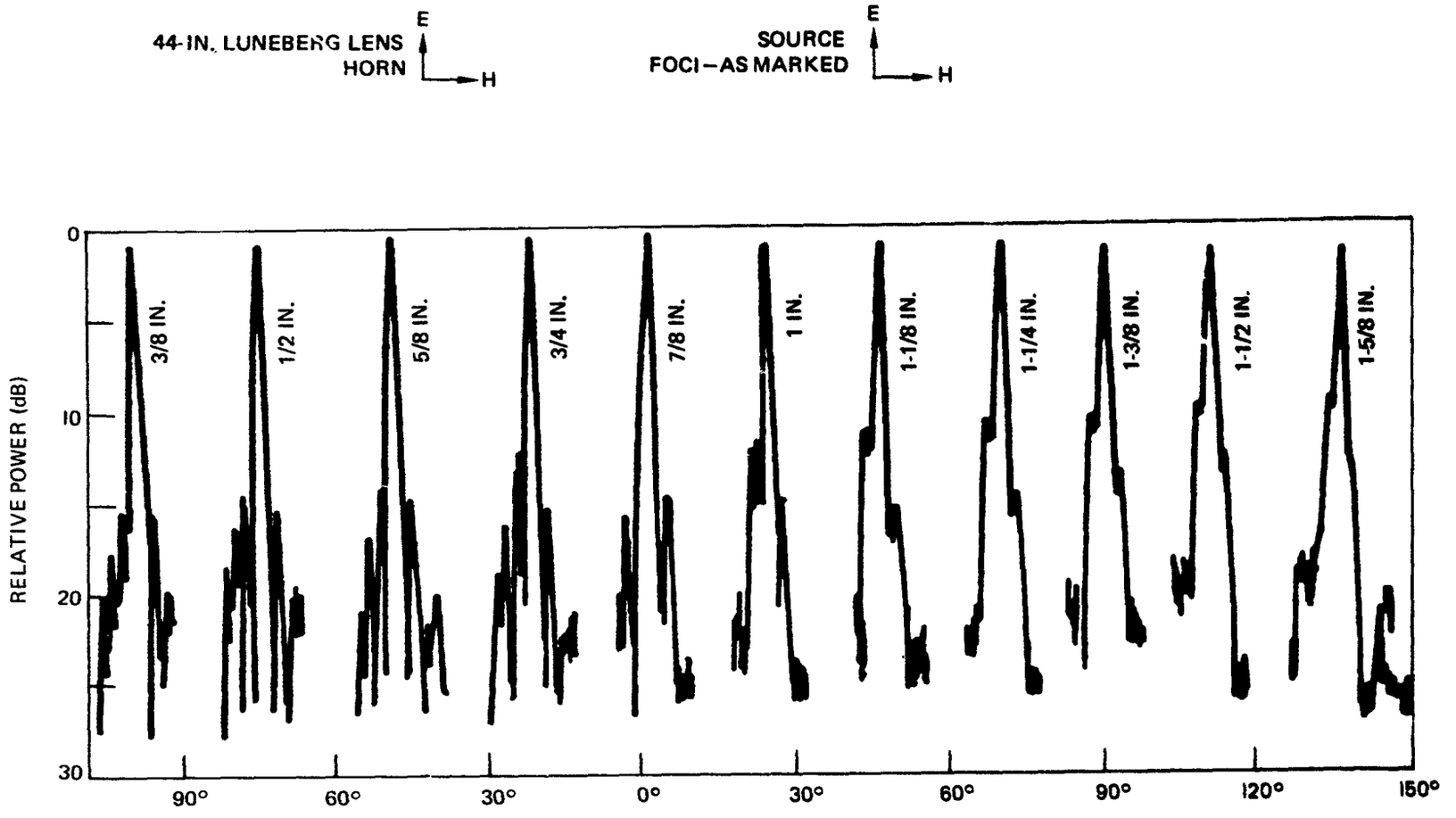

Figure A9. Azimuth patterns at 10 GHz showing change of focus.

Azimuth Response with Feeds at Different Circumferential Spacing

Figure A10 shows patterns for horn 4 with all seven feeds in place. These patterns are similar in main-beam shape and do not exhibit any unusually great sidelobe differences which may be correlated to the difference in horn separation. Figure A11 is a composite pattern of all feeds at both 9° and 12° separation.

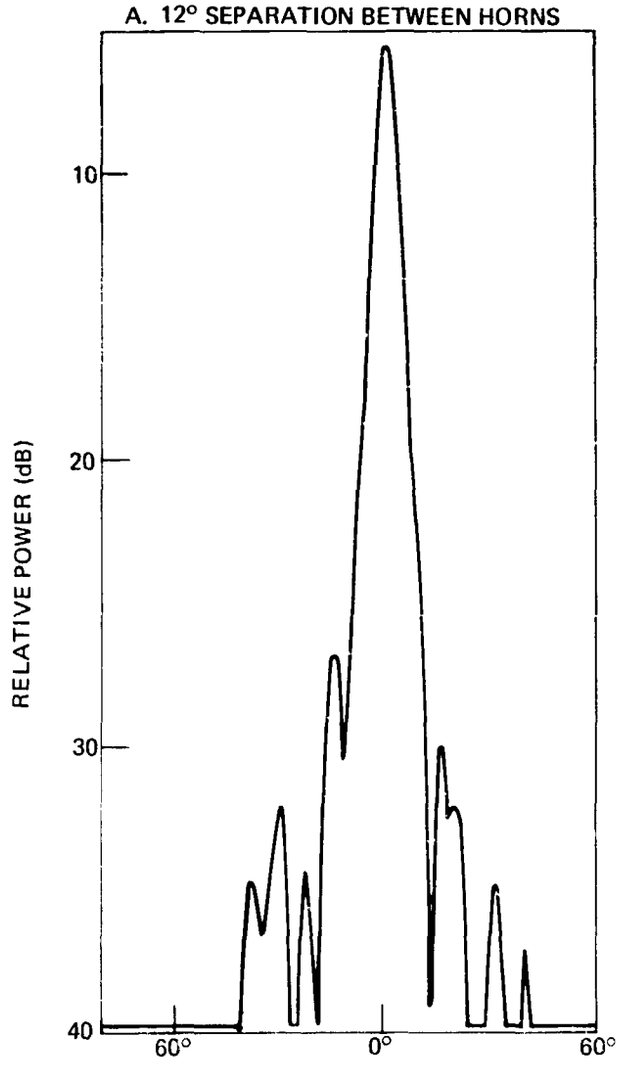

Figure A10 Azimuth patterns at 9 GHz with 18-inch lens for horn 4, shielded and loaded with horizontal polarization

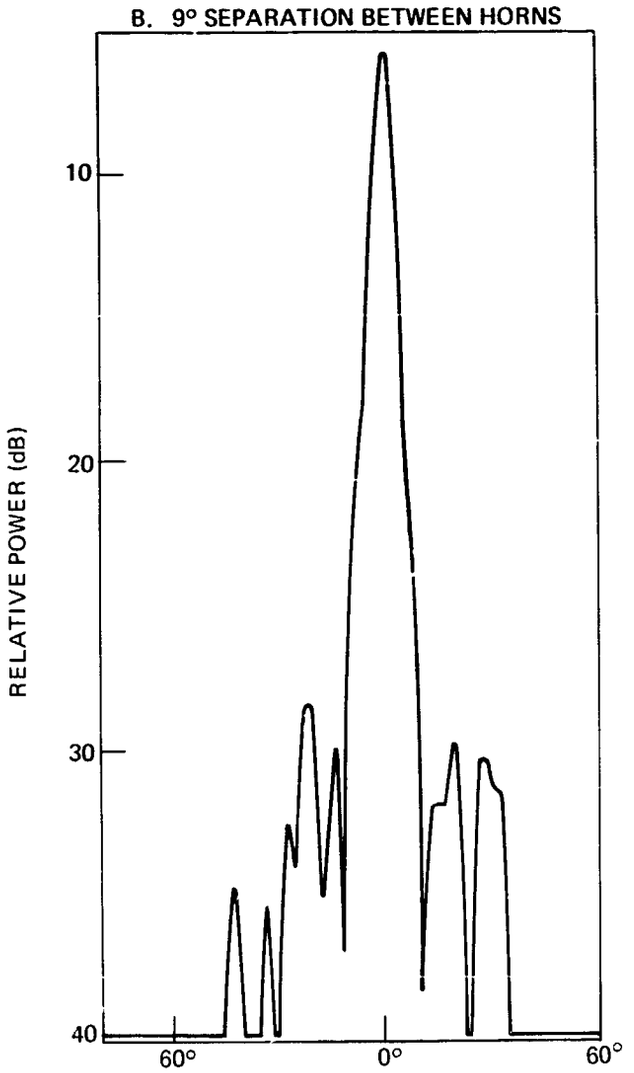

Figure A10. (Continued)

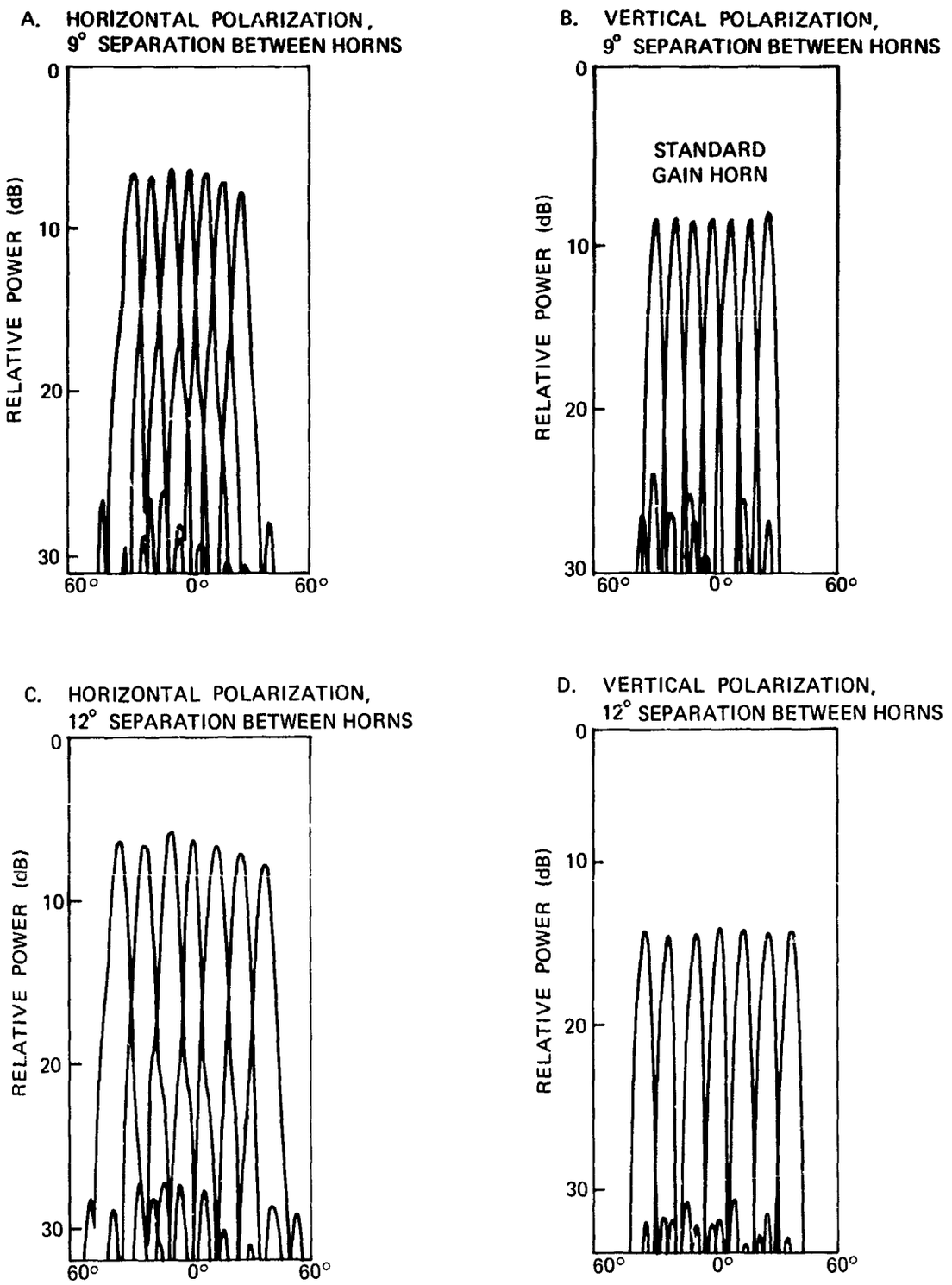

Figure A11. Azimuth patterns at 9 GHz for 18-inch lens for seven feeds, shielded and loaded.

APPENDIX B: IMPLEMENTATION AND PERFORMANCE OF A DF-LENS TEST SYSTEM

Test System Techniques and Objectives

Optimization of the Luneberg and constant-K lenses, involving determination of the capability of each lens to generate high-gain narrowbeams that are close in azimuth, fairly uniform in frequency, and responsive to all polarizations, occupied a major portion of this task. As attention was given to DF-system concepts, it became evident that the lens' beam patterns placed constraints upon the system design and the particular DF technique. Hence, a test system was planned to check these constraints and prove certain system concepts. The major objectives of the test system were as follows:

1. Provide bearing to sources on a pulse-by-pulse basis.
2. Demonstrate a multiple-thresholding technique for extending the dynamic range of each crystal-video channel.
3. Develop logic circuitry to sample all channels energized simultaneously by a single pulse and to indicate bearing by selecting the center sample.
4. Extrapolate the DF performance of a full system using the lens, multiple thresholding, and the pulse-by-pulse BCDL.

The first objective was realized by simultaneously sensing the threshold levels of all channels excited by an rf pulse and by using logic comparators to determine the center channel (or boresight bearing of the source). The logic output denoting the center channel was changed to an analog signal for a Cartesian plot of bearing on a CRT. Figure B1 is a block diagram of the overall technique, showing one channel only. Since this method permits parallel processing of data from all the excited channels, a near real-time display is possible.

The second objective was accomplished, in part, by utilizing two threshold levels at the otuput of each crystal-video channel. Figure B2 shows that any rf signal X dB stronger than the MDS for a given channel would lie between thresholds 1 and 2. A signal $20 + X$ dB stronger would lie above threshold 2 or between thresholds 2 and 3 (if a third threshold were implemented), etc. For a threshold signal impinging directly on one main beam, but looking into the sidelobes of the two adjacent beams (first threshold is broken in all three channels), the BCDL senses the first-threshold output of the three channels simultaneously and selects the bearing of the center beam as boresight to the rf source. If a signal is strong enough to break the second-threshold level in the center channel and only the first-level threshold in the two adjacent channels, the BCDL senses only the second-level threshold of the center channel (first-level threshold outputs are inhibited), and selects the bearing of the center beam as boresight to the rf source. As the signal becomes progressively stronger without exceeding the dynamic range of the lens

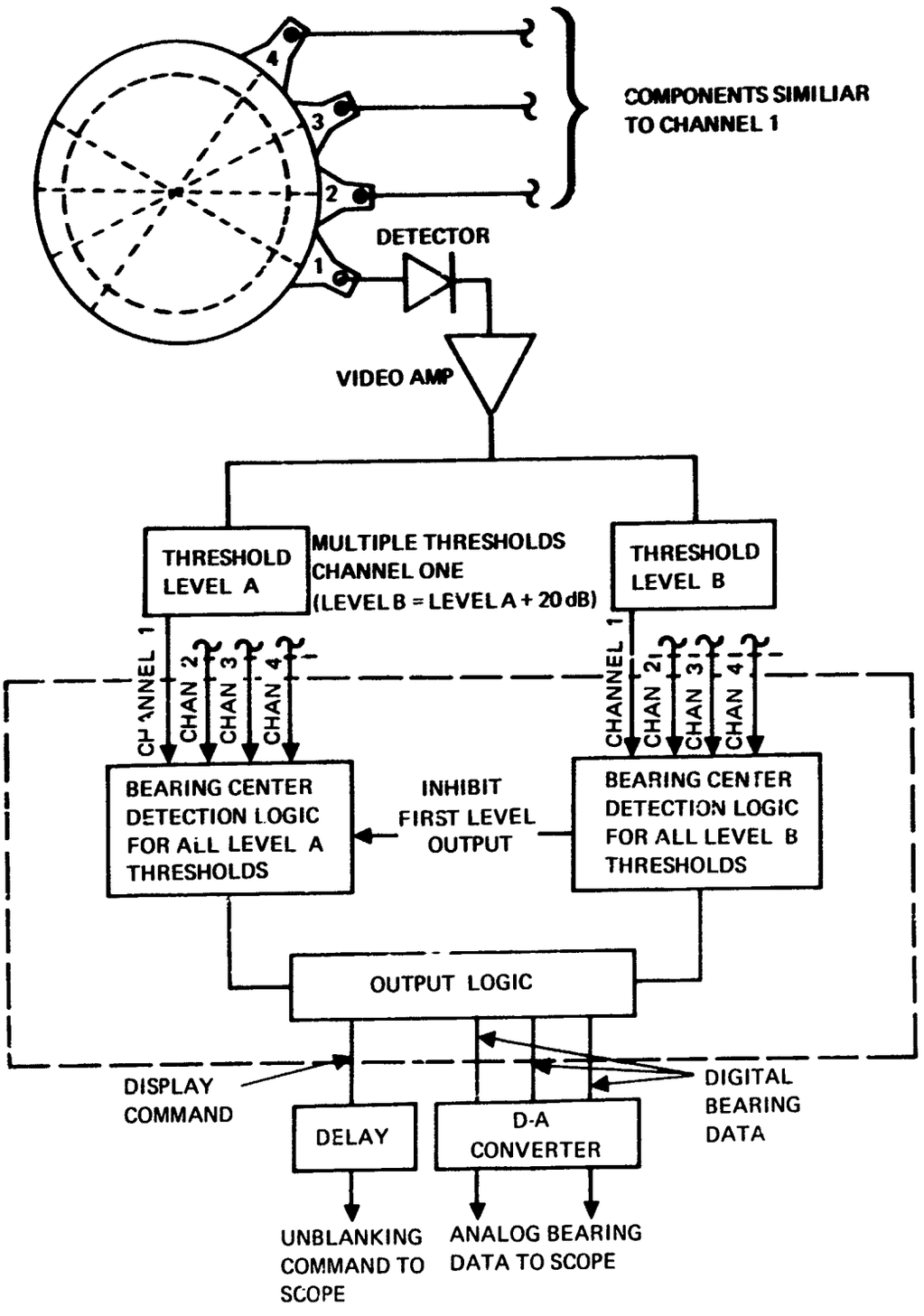

Figure B1. Block diagram for four-channel test system.

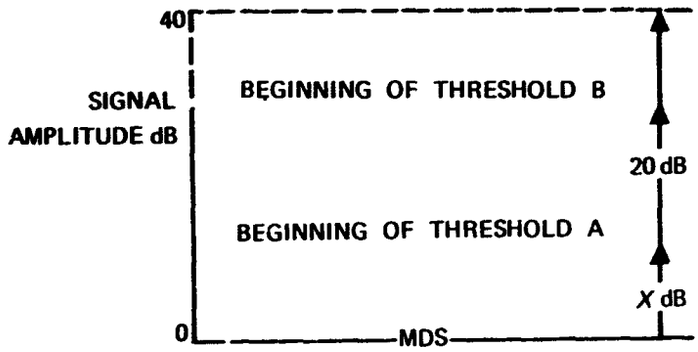

Figure B2. Relative threshold levels for test system (X set to reduce false firings due to noise).

system, it will cause higher threshold responses in those channels nearer boresight so a positive determination of bearing center can be made by the BCDL.

The advantage in this thresholding technique is that sidelobe responses in remote beams are never as high as the main-beam responses at boresight. Hence, sidelobes are ignored by the BCDL, and the antenna system essentially has no sidelobes. Figure B3 shows that a signal 20 + *X* dB above MDS and centered on beam 2 would produce a threshold 2 response in beam 2, and a threshold 1 response in beams 1, 3, and 4. However, the BCDL would ignore the responses in channels 1, 3, and 4, and determine bearing on the basis of the main-beam (higher threshold) response in channel 2. (Note that the response in beam 4 is due to a sidelobe.)

Thresholds for a particular channel output can only be extended to the dynamic range of the crystal. This amounted to about 40 dB in the test system, although newer crystals with up to a 60-dB dynamic range are now being considered. To obtain additional dynamic range for a channel, it is necessary to place an rf divider before the crystal (after the feed horn) so an auxiliary crystal and threshold detector may be added in in parallel. Obviously, some type of crystal protection will be necessary for the crystal which covers the lowest group of thresholds. This can be done with a solid-state limiter and feedback from the higher thresholds to desensitize, or switch out, the lower thresholds during strong signals.

The DF accuracy using the test system can be, at best, ± 4.5° or half the distance between adjacent beam centers. To accomplish this, the BCDL and display were configured to give a between-beam indication for any intercept exciting two (or any even number of adjacent feed horns) adjacent channels to the same threshold level. When three feeds (or any uneven number of feeds) are excited to the same high threshold, the BCDL and display select and indicate the center feed as boresight to the source.

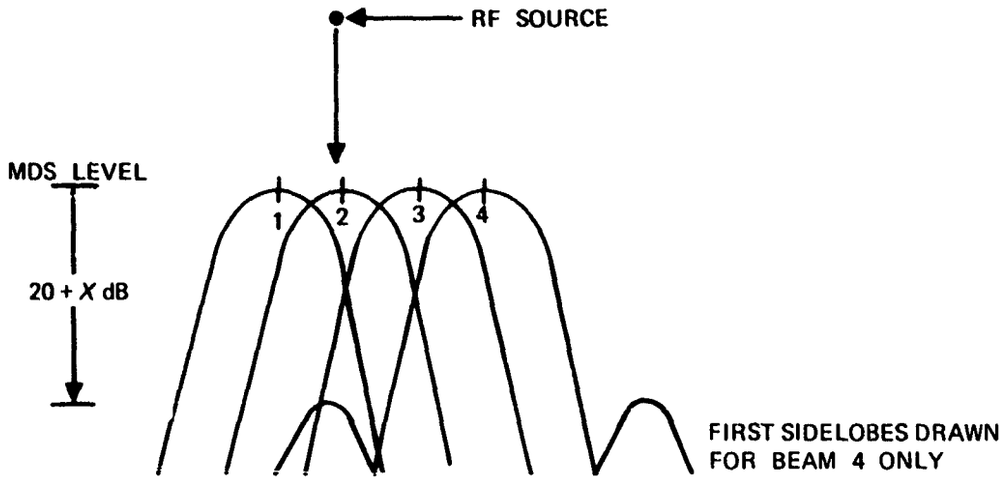

Figure B3 Beam responses showing main beam and remote sidelobe at same azimuth.

Components of the Test System

A test system using the previously described design plan was built to provide reception and bearing determination over an azimuth sector of 27°. It consisted of four crystal-video channels, each feeding a two-level threshold detector permitting a total dynamic range of 40 dB tangential sensitivity. The crystal-video channels were fed by *E*-plane sectoral horns, canted at 45° and spaced 9° apart around the lens. A CRT was used to display bearing. It was marked along the *X*-axis to indicate between-beam and main-beam azimuths for the four horns. Actual signal bearings were indicated by a *Y*-deflection (toward the top of the scope) or dot at the selected azimuth position.

Analyzing Test System Deficiencies

A careful study of the test system reveals certain deficiencies. These can be summarized as follows:

1. Strong signals arriving through the backlobes of feed horns can cause threshold responses in crystal-video channels. (This results in the erroneous display of the reciprocals of the actual bearings for these signals.)

2. Because of the limited dynamic range (40 dB) of the test system, strong sources are able to cause second-level responses in all four channels in spite of being boresighted on the main beam of a single feed horn.

Both of these deficiencies are related to the limited dynamic range between main beam and sidelobes (or backlobes) of the multiple beam patterns.

Although it would be expensive for a test system, the second deficiency can be corrected by extending the system's dynamic range through multiple thresholding, as previously suggested. The first deficiency is more inherent to the design and can only be eliminated by building a system covering 360° azimuth. This would ensure that a signal from any azimuth would always look into a mainlobe as well as a backlobe. As a result, threshold differences would cause the mainlobe response to predominate (break a higher level threshold) and indicate a true bearing to the source.

Figure B4(A) shows the multibeam response (vertical) of the four-channel system* using the Luneberg lens and *E*-plane sectoral feed horns. At crossover between beams 6 and 7, the null depth (from top of main beam) is 7.75 dB. This is approximately 8 dB above the (highest) first sidelobe, which falls at the same azimuth as main beam for beam 7. Sidelobes which fall at the same azimuth as the selected crossover point are considerably farther down. If boresight is taken on beam 7, then the highest (worst case) sidelobe level is down only 15.75 dB from the main beam. This difference is greater than the 7.75 dB between the highest sidelobe level and the crossover null. The smaller value (highest sidelobe to crossover null) is of interest It determines the maximum permissible decibel separation between the first- and second-threshold levels of the test system. This is true because , as signal strength is increased, a signal boresighted at crossover between adjacent beams 6 and 7 to generate a second-level response in the adjacent beams before a first-level response is generated in the sidelobes of a remote beam.

The horizontal patterns, shown in figure B4(B), are better than the vertical patterns. The highest sidelobes are down 19.25 dB from the peak of beam 7. The null depth between beams 6 and 7 is about 6.25 dB. The separation between this null depth and the highest sidelobe is 13 dB. Hence, the maximum permissible decibel separation between the first and second threshold levels would be 13 dB (only 8 dB for the vertical patterns).

The constant-K lens with *E*-plane sectoral horns appears better in this regard than the Luneberg lens. Its beams are broader and apparently cross over nearer the peaks than do those of the Luneberg, while the sidelobe level remains low. This results in a greater separation between null depth and first sidelobes, thereby permitting a greater spread between the individual threshold levels. The remote focus of the constant-K lens is a factor too. It permits the feed horns to be placed closer than 9° to obtain crossover between adjacent beams near the peaks.

An optimum multibeam pattern would be one in which the null depth at crossover between adjacent beams is minimum (near peaks of main beams), and all sidelobes levels are minimum. Consequently, the decibel separation between the null depth and the first sidelobe levels would be maximized. The advantage would be that for a desired receiver-dynamic range, fewer thresholds per channel would be required

---

* *Only beams 4, 5, 6, and 7 were used for the four-channel test system They were numbered consecutively 1 through 4, where beam 4 corresponded to channel 1*

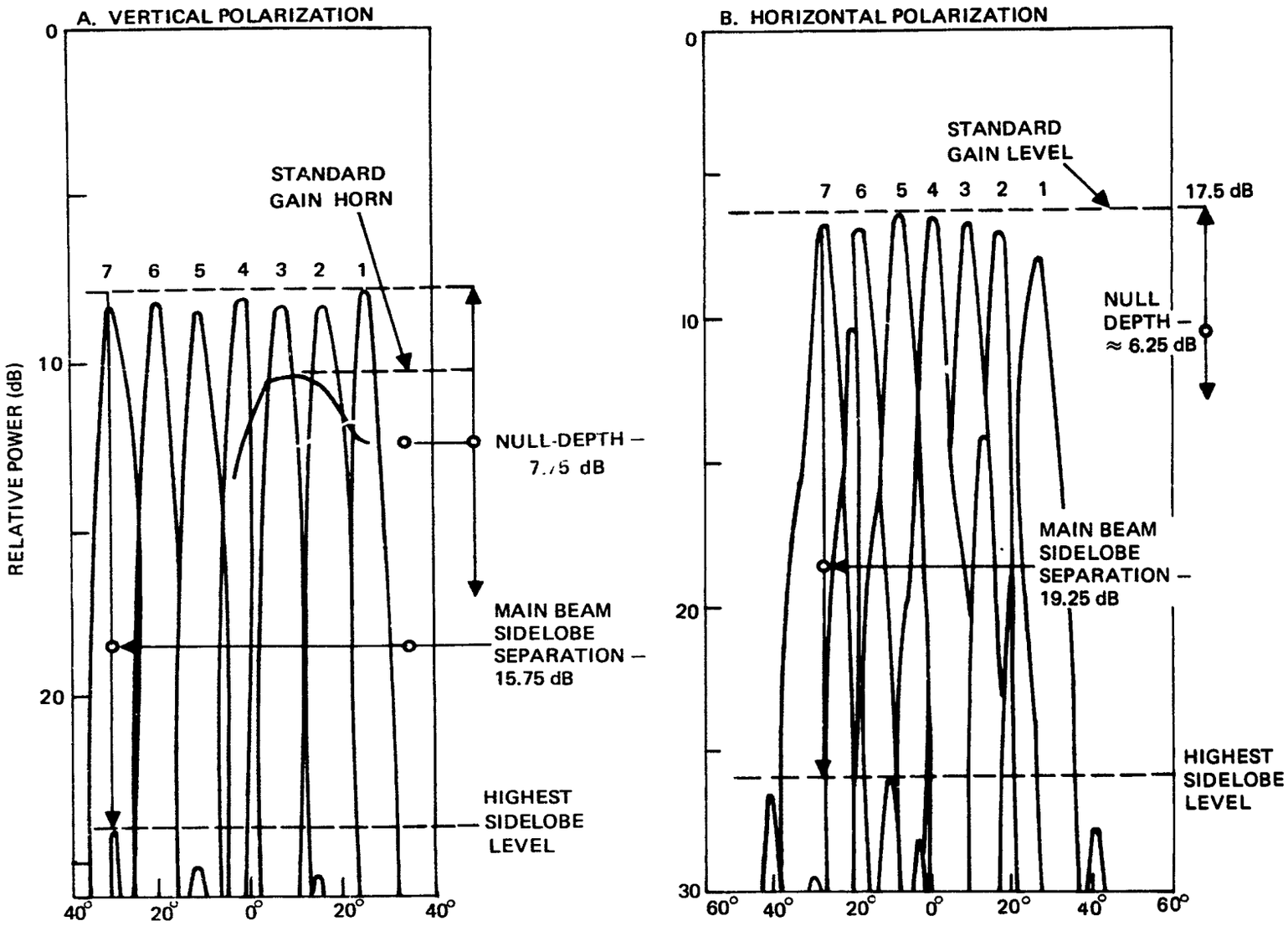

Figure B4. Azimuth patterns at 9 GHz with 18-inch lens for seven feeds, loaded and shielded, with 9° separation between horns (marked to show parameters of interest in test system).

Testing the System

It was advantageous, in terms of cost, to build only the limited two-threshold-level test system described in the preceding section. To obtain useful results, controlled tests were run in an anechoic chamber. This permitted controlled illumination of the frontlobes of the feed horns through the lens, which avoided backlobe patterns. In addition, the power level of the source could be easily adjusted to any acceptable level within the system's dynamic range, thereby avoiding threshold problems between main beams and sidelobes of remote beams.

An optimum power setting was found to be one which excited first-level threshold responses in adjacent beams at crossover without also exciting a simultaneous first-level response in a remote beam. This was particularly important during the tests, since the actual thresholds had been set 20 dB apart instead of only 8 dB as dictated by the beam patterns. Had the power been set higher and the signal boresighted at crossover between beams 6 and 7, a remote beam (*e.g.*, channel 4) would register a first-level response before a second-level response would be excited in beams 6 and 7. This would confuse the BCDL, and the bearing display would be erroneous.

The anechoic chamber was approximately 20-feet long. It contained a rotatable mount which permitted boresighting the fixed source at any bearing in the usable sector of the antenna. This enabled checking the DF performance as follows:

1. The center bearing of each feed horn was marked in the X-direction on the face of the CRT along with the beam-crossover bearings.

2. Source was sequentially boresighted on each feed horn, and the display was observed to see if a dot appeared on the CRT at the proper positions.

3. The antenna was rotated slowly, but continuously, so the source could illuminate the entire sector, thereby simulating a moving source.

The CRT display was observed to track properly giving center-beam and crossover point bearings. Typical multiple exposure photographs of these results are shown in figure B5.

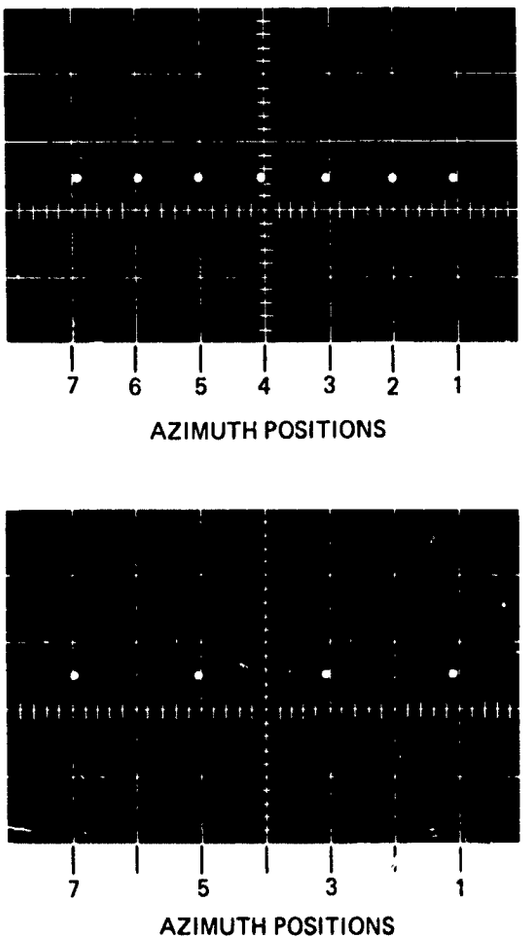

Figure B5. Typical bearing displays showing multiple exposure of intercepts at various azimuth positions.

UNCLASSIFIED
Security Classification

DOCUMENT CONTROL DATA - R & D

(Security classification of title, body of abstract and indexing annotation must be entered when the overall report is classified)

1 ORIGINATING ACTIVITY *(Corporate author)* Naval Electronics Laboratory Center San Diego, California 92152	2a. REPORT SECURITY CLASSIFICATION UNCLASSIFIED 2b GROUP

3 REPORT TITLE

LUNEBERG LENS ANTENNA – TESTING FOR ECM APPLICATION

4 DESCRIPTIVE NOTES *(Type of report and inclusive dates)*

Research and Development — March 1967 - April 1968

5 AUTHOR(S) *(First name, middle initial, last name)*

M. B. Bryant and B. R. Hunt

6 REPORT DATE	7a. TOTAL NO OF PAGES	7b NO OF REFS
1 April 1969	71	5

8a CONTRACT OR GRANT NO	9a ORIGINATOR'S REPORT NUMBER(S) 1621
b PROJECT NO SF11.151.001 c. Task 09251 (NELC G203) d.	9b OTHER REPORT NO(S) *(Any other numbers that may be assigned this report)*

10 DISTRIBUTION STATEMENT

Each transmittal of this document outside the agencies of the U. S. Government must have prior approval of NELC.

11 SUPPLEMENTARY NOTES	12 SPONSORING MILITARY ACTIVITY
	SHIPS 03522

13 ABSTRACT

The Luneberg lens was investigated for use as an *X*-band antenna capable of providing high gain, narrow beamwidths, and low sidelobes that are comparatively better than those furnished by other microwave-ECM antennas. The multibeam capability of the lens was optimized and explored for direction-finding system application. A constant-K lens was also designed for comparative purposes and evaluated as part of the task.

DD FORM 1 NOV 65 1473 (PAGE 1)

S/N 0101-807-6801

UNCLASSIFIED
Security Classification

14 KEY WORDS	LINK A		LINK B		LINK C	
	ROLE	WT	ROLE	WT	ROLE	WT
Luneberg lenses – Applications						
ECM equipment						
Direction-finding antennas						